



This is a repository copy of *The gene cortex controls mimicry and crypsis in butterflies and moths* .

White Rose Research Online URL for this paper:
<http://eprints.whiterose.ac.uk/98941/>

Version: Accepted Version

Article:

Nadeau, N.J. orcid.org/0000-0002-9319-921X, Pardo-Diaz, C., Whibley, A. et al. (16 more authors) (2016) The gene cortex controls mimicry and crypsis in butterflies and moths. Nature, 534. pp. 106-110. ISSN 0028-0836

<https://doi.org/10.1038/nature17961>

Reuse

Unless indicated otherwise, fulltext items are protected by copyright with all rights reserved. The copyright exception in section 29 of the Copyright, Designs and Patents Act 1988 allows the making of a single copy solely for the purpose of non-commercial research or private study within the limits of fair dealing. The publisher or other rights-holder may allow further reproduction and re-use of this version - refer to the White Rose Research Online record for this item. Where records identify the publisher as the copyright holder, users can verify any specific terms of use on the publisher's website.

Takedown

If you consider content in White Rose Research Online to be in breach of UK law, please notify us by emailing eprints@whiterose.ac.uk including the URL of the record and the reason for the withdrawal request.



eprints@whiterose.ac.uk
<https://eprints.whiterose.ac.uk/>

A major gene controls mimicry and crypsis in butterflies and moths

Nicola J. Nadeau^{1,2}, Carolina Pardo-Diaz³, Annabel Whibley^{4,5}, Megan Supple^{2,6}, Suzanne V. Saenko⁴, Richard W. R. Wallbank^{2,7}, Grace C. Wu⁸, Luana Maroja⁹, Laura Ferguson¹⁰, Joseph J. Hanly^{2,7}, Heather Hines¹¹, Camilo Salazar³, Richard Merrill^{2,7}, Andrea Dowling¹², Richard ffrench-Constant¹², Violaine Llaurens⁴, Mathieu Joron⁴, W. Owen McMillan², Chris D. Jiggins^{7,2}

¹Department of Animal and Plant Sciences, University of Sheffield, UK; ²Smithsonian Tropical Research Institute, Panama; ³Biology Program, Faculty of Natural Sciences and Mathematics. Universidad del Rosario. Cra. 24 No 63C-69, Bogotá D.C., 111221, Colombia; ⁴Institut de Systématique, Evolution et Biodiversité (UMR 7205 CNRS, MNHN, UPMC, EPHE, Sorbonne Université), Museum National d'Histoire Naturelle, CP50, 57 rue Cuvier, 75005 PARIS, France; ⁵Cell and Developmental Biology, John Innes Centre, Norwich, UK, NR4 7UH; ⁶The Australian National University, ACT, Australia; ⁷Department of Zoology, University of Cambridge, UK; ⁸Energy and Resources Group, University of California at Berkeley, CA, USA; ⁹Department of Biology, Williams College, MA, USA; ¹⁰Department of Zoology, University of Oxford, UK; ¹¹ Penn State University, 517 Mueller, University Park, PA 16802; ¹²School of Biosciences, University of Exeter in Cornwall, Penryn, UK TR10 9EZ

The wing patterns of butterflies and moths (Lepidoptera) are diverse and striking examples of evolutionary diversification by natural selection^{1,2}. Lepidopteran wing colour patterns are a key innovation, consisting of arrays of coloured scales. We still lack a general understanding of how these patterns are controlled and if there is any commonality across the 160,000 moth and 17,000 butterfly species. Here, we identify a gene, *cortex*, through fine-scale mapping using population genomics and gene expression analyses, which regulates pattern switches in multiple species across the mimetic radiation in *Heliconius* butterflies. *cortex* belongs to a fast evolving subfamily of the otherwise highly conserved *fizzy* family of cell cycle regulators³, suggesting that it most likely regulates pigmentation patterning through regulation of scale cell development. In parallel with findings in the peppered moth (*Biston betularia*)⁴, our results suggest that this mechanism is common within Lepidoptera and that *cortex* has become a major target for natural selection acting on colour and pattern variation in this group of insects.

In *Heliconius*, there is a major effect locus, *Yb*, that controls a diversity of colour pattern elements across the genus. It is the only locus in *Heliconius* that regulates all scale types and colours, including the diversity of white and yellow pattern elements in the two co-mimics *H. melpomene* (Hm) and *H. erato* (He), but also whole wing variation in black, yellow, white, and orange/red elements in *H. numata* (Hn)⁵⁻⁷. In addition, genetic variation underlying the Bigeye wing pattern mutation in *Bicyclus anynana*, melanism in the peppered moth, *Biston betularia*, and melanism and patterning differences in the silkworm, *Bombyx mori*, have all been localised to homologous genomic regions⁸⁻¹⁰ (Fig 1). Therefore, this genomic region appears to contain one or more genes that act as major regulators of wing pigmentation and patterning across the Lepidoptera.

Previous mapping of this locus in He, Hm and Hn identified a genomic interval of ~1Mb¹¹⁻¹³ (Extended Data Table 1), which also overlaps with the 1.4Mb region containing the carbonaria locus in *B. betularia*⁹ and a 100bp non-coding region containing the Ws mutation in *B. mori*¹⁰ (Fig 1). We took a population genomics approach to identify single nucleotide polymorphisms (SNPs) most strongly associated with phenotypic variation within the ~1Mb Heliconius interval. The diversity of wing patterning in Heliconius arises from divergence at wing pattern loci⁷, while convergent patterns generally involve the same loci and sometimes even the same alleles¹⁴⁻¹⁶. We used this pattern of divergence and sharing to identify SNPs associated with colour pattern elements across many individuals from a wide diversity of colour pattern phenotypes (Fig 2).

In three separate Heliconius species, our analysis consistently implicated the gene cortex as being involved in adaptive differences in wing colour pattern. In He the strongest associations with the presence of a yellow hindwing bar were centred around the genomic region containing cortex (Fig 2A). We identified 108 SNPs that were fixed for one allele in He favorinus, and fixed for the alternative allele in all individuals lacking the yellow bar, the majority of which were in introns of cortex (Extended Data Table 2). 15 SNPs showed a similar fixed pattern for He demophoon, which also has a yellow bar. These were non-overlapping with those in He favorinus, consistent with the hypothesis that this phenotype evolved independently in the two disjunct populations¹⁷.

Previous work has suggested that alleles at the Yb locus are shared between Hm and the closely related species *H. timareta*, and also the more distantly related species *H. elevatus*, resulting in mimicry between these species¹⁸. Across these species, the strongest associations with the yellow hindwing bar phenotype were again found at cortex (Fig 2D, Extended Data Fig 1A and Table 3). Similarly, the strongest associations with the yellow forewing band were found around the 5' UTRs of cortex and gene HM00036, an orthologue of D.

melanogaster washout gene. A single SNP ~17kb upstream of cortex (the closest gene) was perfectly associated with the yellow forewing band across all Hm, *H. timareta* and *H. elevatus* individuals (Extended Data Fig 1A, Fig 2 and Table 3). We found no fixed coding sequence variants at cortex in a larger sample (43-61 individuals) of *Hm aglaope* and *Hm amaryllis* (Extended Data Figure 3, Supplementary Information), which differ in Yb controlled phenotypes¹⁹, suggesting that functional variants are likely to be regulatory rather than coding. We found extensive transposable element variation around cortex but it is unclear if any of these associate with phenotype (Extended Data Figure 3 and Table 4; Supplementary Information).

Finally, in Hn large inversions at the P supergene locus (Fig 1) are associated with different morphs¹³. There is a steep increase in genotype-by-phenotype association at the breakpoint of inversion 1, consistent with the role of these inversions in reducing recombination (Fig 2E). However, the *bicoloratus* morph can recombine with all other morphs across one or the other inversion, permitting finer-scale association mapping of this region. As in He and Hm, this analysis showed a narrow region of associated SNPs corresponding exactly to the cortex gene (Fig 2E), again with the majority of SNPs in introns (Extended Data Table 2). This associated region does not correspond to any other known genomic feature, such as an inversion or inversion breakpoint.

To determine whether sequence variants around cortex were regulating its expression we investigated gene expression across the Yb locus. We used a custom designed microarray including probes from all predicted genes in the *H. melpomene* genome¹⁸, as well as probes tiled across the central portion of the Yb locus, focussing on two naturally hybridising Hm races (*plesseni* and *malleti*) that differ in Yb controlled phenotypes⁷. cortex was the only gene across the entire interval to show significant expression differences both between races with different wing patterns and between wing sections with different pattern elements (Fig 3).

This finding was reinforced in the tiled probe set, where we observed strong differences in expression of cortex exons and introns but few differences outside this region (Extended Data Table 2). cortex expression was higher in *Hm malleti* than *Hm plesseni* in all three wing sections used (but not eyes) (Fig 3C; Extended Data Fig 4C). When different wing sections were compared within each race, cortex expression in *Hm malleti* was higher in the distal section that contains the Yb controlled yellow forewing band, consistent with cortex producing this band. In contrast, *Hm plesseni*, which lacks the yellow band, had higher cortex expression in the proximal forewing section (Fig 3F; Extended Data Fig 4J). Expression differences were found only in day 1 and day 3 pupal wings rather than day 5 or day 7 (Extended Data Fig 4), similar to the pattern observed previously for the transcription factor *optix*²⁰.

Differential expression was not confined to the exons of cortex; the majority of differentially expressed probes in the tiling array corresponded to cortex introns (Fig 3). This does not appear to be due to transposable element variation (Extended Data Table 2), but may be due to elevated background transcription and unidentified splice variants. RT-PCR revealed a diversity of splice variants (Extended Data Fig 5), and sequenced products revealed 8 non-constitutive exons and 6 variable donor/acceptor sites, but this was not exhaustive (Supplementary Information). We cannot rule out the possibility that some of the differentially expressed intronic regions could be distinct non-coding RNAs. However, qRT-PCR in other hybridising races with divergent Yb alleles (*aglaope/amaryllis* and *rosina/melpomene*) also identified expression differences at cortex and allele-specific splicing differences between both pairs of races (Extended Data Figs 1 and 5, Supplementary Information).

Finally, in situ hybridisation of cortex in final instar larval hindwing discs showed expression in wing regions fated to become black in the adult wing, most strikingly in their

correspondence to the black patterns on adult Hn wings (Fig 4). In contrast, the array results from pupal wings were suggestive of higher expression in non-melanic regions. This may suggest that cortex is upregulated at different time-points in wing regions fated to become different colours.

Overall, cortex shows significant differential expression and is the only gene in the candidate region to be consistently differentially expressed in multiple race comparisons and between differently patterned wing regions. Coupled with the strong genotype-by-phenotype associations across multiple independent lineages (Extended Data Table 1), this strongly implicates cortex as a major regulator of colour and pattern. However, we have not excluded the possibility that other genes in this region also influence pigmentation patterning. A prominent role for cortex is also supported by studies in other taxa; our identification of distant 5' untranslated exons of cortex (Supplementary Information) suggests that the 100bp interval containing the Ws mutation in *B. mori* is likely to be within an intron of cortex and not in intergenic space as previously thought¹⁰. In addition, fine-mapping and gene expression also implicate cortex as controlling melanism in the peppered moth⁴.

It seems likely that cortex controls pigmentation patterning through control of scale cell development. The cortex gene falls in an insect specific lineage within the fizzy/CDC20 family of cell cycle regulators (Extended Data Fig 6A). The phylogenetic tree of the gene family highlighted three major orthologous groups, two of which have highly conserved functions in cell cycle regulation mediated through interaction with the anaphase promoting complex/cyclosome (APC/C)^{3,21}. The third group, cortex, is evolving rapidly, with low amino acid identity between *D. melanogaster* and Hm cortex (14.1%), contrasting with much higher identities for orthologues between these species in the other two groups (fzy, 47.8% and rap/fzr, 47.2%, Extended Data Fig 6A). *Drosophila melanogaster* cortex acts through a

similar mechanism to *fzy* in order to control meiosis in the female germ line^{22–24}. Hm cortex also has some conservation of the fizzy family C-box and IR elements (Supplementary Information) that mediate binding to the APC/C²³, suggesting that it may have retained a cell cycle function, although we found that expressing Hm cortex in *D. melanogaster* wings produced no detectable effect (Extended Data Fig 6, Supplementary Information).

Previously identified butterfly wing patterning genes have been transcription factors or signalling molecules^{20,25}. Developmental rate has long been thought to play a role in lepidopteran patterning^{26,27}, but cortex was not a likely a priori candidate, because its *Drosophila* orthologue has a highly specific function in meiosis²³. The recruitment of cortex to wing patterning appears to have occurred before the major diversification of the Lepidoptera and this gene has repeatedly been targeted by natural selection^{1,7,9,28} to generate both cryptic⁴ and aposematic patterns.

References

1. Cook, L. M., Grant, B. S., Saccheri, I. J. & Mallet, J. Selective bird predation on the peppered moth: the last experiment of Michael Majerus. *Biol. Lett.* **8**, 609–612 (2012).
2. Jiggins, C. D. Ecological Speciation in Mimetic Butterflies. *BioScience* **58**, 541–548 (2008).
3. Dawson, I. A., Roth, S. & Artavanis-Tsakonas, S. The *Drosophila* Cell Cycle Gene *fizzy* Is Required for Normal Degradation of Cyclins A and B during Mitosis and Has Homology to the CDC20 Gene of *Saccharomyces cerevisiae*. *J. Cell Biol.* **129**, 725–737 (1995).
4. Van't Hof, A. E. et al. The industrial melanism mutation in British peppered moths is a transposable element. *Nature* **This issue**,

- 166 5. Joron, M. et al. A Conserved Supergene Locus Controls Colour Pattern Diversity in
167 *Heliconius* Butterflies. *PLoS Biol.* **4**, (2006).
- 168 6. Sheppard, P. M., Turner, J. R. G., Brown, K. S., Benson, W. W. & Singer, M. C.
169 Genetics and the Evolution of Muellierian Mimicry in *Heliconius* Butterflies. *Philos.*
170 *Trans. R. Soc. Lond. B. Biol. Sci.* **308**, 433–610 (1985).
- 171 7. Nadeau, N. J. et al. Population genomics of parallel hybrid zones in the mimetic
172 butterflies, *H. melpomene* and *H. erato*. *Genome Res.* **24**, 1316–1333 (2014).
- 173 8. Beldade, P., Saenko, S. V., Pul, N. & Long, A. D. A Gene-Based Linkage Map for
174 *Bicyclus anynana* Butterflies Allows for a Comprehensive Analysis of Synteny with the
175 Lepidopteran Reference Genome. *PLoS Genet* **5**, e1000366 (2009).
- 176 9. van't Hof, A. E., Edmonds, N., Dalíková, M., Marec, F. & Saccheri, I. J. Industrial
177 Melanism in British Peppered Moths Has a Singular and Recent Mutational Origin.
178 *Science* **332**, 958 –960 (2011).
- 179 10. Ito, K. et al. Mapping and recombination analysis of two moth colour mutations, Black
180 moth and Wild wing spot, in the silkworm *Bombyx mori*. *Heredity* (2015).
181 doi:10.1038/hdy.2015.69
- 182 11. Counterman, B. A. et al. Genomic Hotspots for Adaptation: The Population Genetics of
183 Müllerian Mimicry in *Heliconius erato*. *PLoS Genet.* **6**, e1000796 (2010).
- 184 12. Ferguson, L. et al. Characterization of a hotspot for mimicry: assembly of a butterfly
185 wing transcriptome to genomic sequence at the HmYb/Sb locus. *Mol. Ecol.* **19**, 240–254
186 (2010).
- 187 13. Joron, M. et al. Chromosomal rearrangements maintain a polymorphic supergene
188 controlling butterfly mimicry. *Nature* **477**, 203–206 (2011).
- 189 14. Hines, H. M. et al. Wing patterning gene redefines the mimetic history of *Heliconius*
190 butterflies. *Proc. Natl. Acad. Sci.* **108**, 19666–19671 (2011).

- 191 15. Pardo-Diaz, C. et al. Adaptive Introgression across Species Boundaries in *Heliconius*
 192 Butterflies. *PLoS Genet* **8**, e1002752 (2012).
- 193 16. Wallbank, R. W. R. et al. Evolutionary Novelty in a Butterfly Wing Pattern through
 194 Enhancer Shuffling. *PLoS Biol* **14**, e1002353 (2016).
- 195 17. Maroja, L. S., Alschuler, R., McMillan, W. O. & Jiggins, C. D. Partial Complementarity
 196 of the Mimetic Yellow Bar Phenotype in *Heliconius* Butterflies. *PLoS ONE* **7**, e48627
 197 (2012).
- 198 18. The *Heliconius* Genome Consortium. Butterfly genome reveals promiscuous exchange of
 199 mimicry adaptations among species. *Nature* **487**, 94–98 (2012).
- 200 19. Mallet, J. The Genetics of Warning Colour in Peruvian Hybrid Zones of *Heliconius erato*
 201 and *H. melpomene*. *Proc. R. Soc. Lond. B Biol. Sci.* **236**, 163–185 (1989).
- 202 20. Reed, R. D. et al. optix Drives the Repeated Convergent Evolution of Butterfly Wing
 203 Pattern Mimicry. *Science* **333**, 1137–1141 (2011).
- 204 21. Barford, D. Structural insights into anaphase-promoting complex function and
 205 mechanism. *Philos. Trans. R. Soc. B Biol. Sci.* **366**, 3605–3624 (2011).
- 206 22. Chu, T., Henrion, G., Haegeli, V. & Strickland, S. Cortex, a *Drosophila* gene required to
 207 complete oocyte meiosis, is a member of the Cdc20/fizzy protein family. *genesis* **29**,
 208 141–152 (2001).
- 209 23. Pesin, J. A. & Orr-Weaver, T. L. Developmental Role and Regulation of cortex, a
 210 Meiosis-Specific Anaphase-Promoting Complex/Cyclosome Activator. *PLoS Genet* **3**,
 211 e202 (2007).
- 212 24. Swan, A. & Schüpbach, T. The Cdc20/Cdh1-related protein, Cort, cooperates with
 213 Cdc20/Fzy in cyclin destruction and anaphase progression in meiosis I and II in
 214 *Drosophila*. *Dev. Camb. Engl.* **134**, 891–899 (2007).

- 215 25. Martin, A. et al. Diversification of complex butterfly wing patterns by repeated
216 regulatory evolution of a Wnt ligand. *Proc. Natl. Acad. Sci.* **109**, 12632–12637 (2012).
- 217 26. Koch, P. B., Lorenz, U., Brakefield, P. M. & ffrench-Constant, R. H. Butterfly wing
218 pattern mutants: developmental heterochrony and co-ordinately regulated phenotypes.
219 *Dev. Genes Evol.* **210**, 536–544 (2000).
- 220 27. Gilbert, L. E., Forrest, H. S., Schultz, T. D. & Harvey, D. J. Correlations of ultrastructure
221 and pigmentation suggest how genes control development of wing scales of *Heliconius*
222 butterflies. *J. Res. Lepidoptera* **26**, 141–160 (1988).
- 223 28. Mallet, J. & Barton, N. H. Strong Natural Selection in a Warning-Color Hybrid Zone.
224 *Evolution* **43**, 421–431 (1989).
- 225 29. Wahlberg, N., Wheat, C. W. & Peña, C. Timing and Patterns in the Taxonomic
226 Diversification of Lepidoptera (Butterflies and Moths). *PLoS ONE* **8**, e80875 (2013).
- 227 30. Surridge, A. et al. Characterisation and expression of microRNAs in developing wings of
228 the neotropical butterfly *Heliconius melpomene*. *BMC Genomics* **12**, 62 (2011).

230 **Supplementary Information** is linked to the online version of the paper at

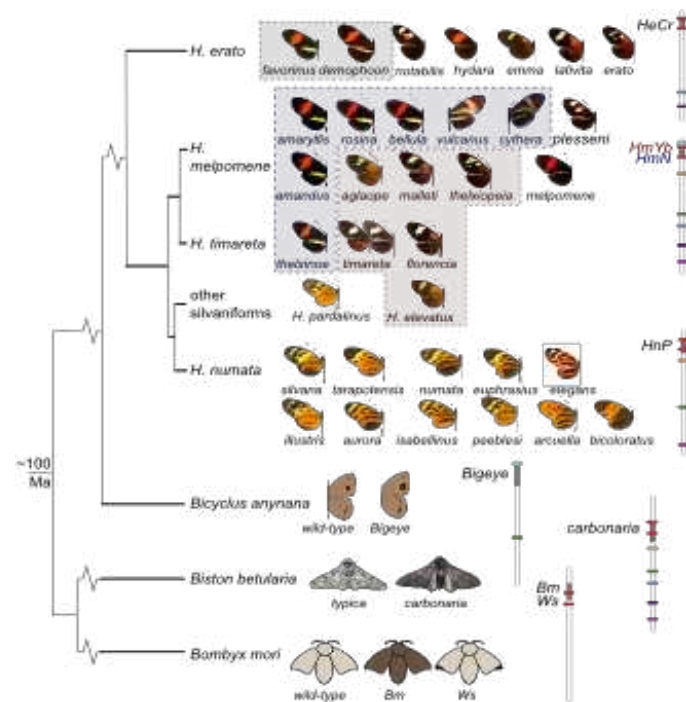
231 www.nature.com/nature.

232 **Acknowledgements** We thank Christopher Saski, Clemson University, for assembly of the
233 He BACs. Moises Abanto and Adriana Tapia assisted with raising butterflies. Thanks to
234 Mathieu Chouteau, Jake Morris and Kanchon Dasmahapatra for providing larvae for in situ
235 hybridisations. Anna Morrison, Robert Tetley, Sarah Carl and Hanna Wegener assisted with
236 lab work at the University of Cambridge. Simon Baxter made the Hm fosmid libraries. We
237 thank the governments of Colombia, Ecuador, Panama and Peru for permission to collect
238 butterflies. This work was funded by a Leverhulme Trust award and BBSRC grant
239 (H01439X/1) to CDJ, NSF grants (DEB 1257689, IOS 1052541) to WOM, an ERC starting

grant to MJ and a French National Agency for Research (ANR) grant to VL (ANR-13-JSV7-0003-01). NJN is funded by a NERC fellowship (NE/K008498/1).

Author Contributions NJN performed the association analyses, 5' RACE, RT-PCR, qRT-PCR and prepared the manuscript. NJN and CDJ co-ordinated the research. CP-D performed and analysed the microarray and RNAseq experiments. AW performed the Hn association analysis. MS assembled and annotated the HeCr BAC reference and the He alignments. SVS performed in situ hybridizations. RWRW performed the transgenic experiments and analysis of de novo assembled sequences and fosmids together with JJH. GW and LF initially identified splicing variants of cortex. LM performed crosses between Hm races. HH screened the HeCr BAC library. CS and RM provided samples. AD contributed to the Hm BAC sequencing and annotation. R-fC, MJ, VL, WOM and CDJ are PIs who obtained funding and led the project elements. All authors commented on the manuscript.

Author Information Short read sequence data generated for this study are available from ENA (<http://www.ebi.ac.uk/ena>) under study accession PRJEB8011 and PRJEB12740 (see Supplementary Table 1 for previously published data accessions). The updated Cr contig is deposited in Genbank with accession KC469893. The assembled Hm fosmid sequences are deposited in Genbank with accessions KU514430-KU514438. The microarray data are deposited in GEO with accessions GSM1563402- GSM1563497. Reprints and permissions information is available at www.nature.com/reprints. Correspondence and requests for materials should be addressed to n.nadeau@sheffield.ac.uk or c.jiggins@zoo.cam.ac.uk



264

265 Figure 1. A homologous genomic region controls a diversity of phenotypes across the
 266 Lepidoptera. Left: phylogenetic relationships²⁹. Right: chromosome maps with colour pattern
 267 intervals in grey, coloured bars represent markers used to assign homology^{5,8-10}, the first and
 268 last genes from Fig 2 shown in red. In He the HeCr locus controls the yellow hind-wing bar
 269 phenotype (grey boxed races). In Hm it controls both the yellow hind-wing bar (HmYb, pink
 270 box) and the yellow forewing band (HmN, blue box). In Hn it modulates black, yellow and
 271 orange elements on both wings (HnP), producing phenotypes that mimic butterflies in the
 272 genus Melinaea. Morphs/races of Heliconius species included in this study are shown with
 273 names.

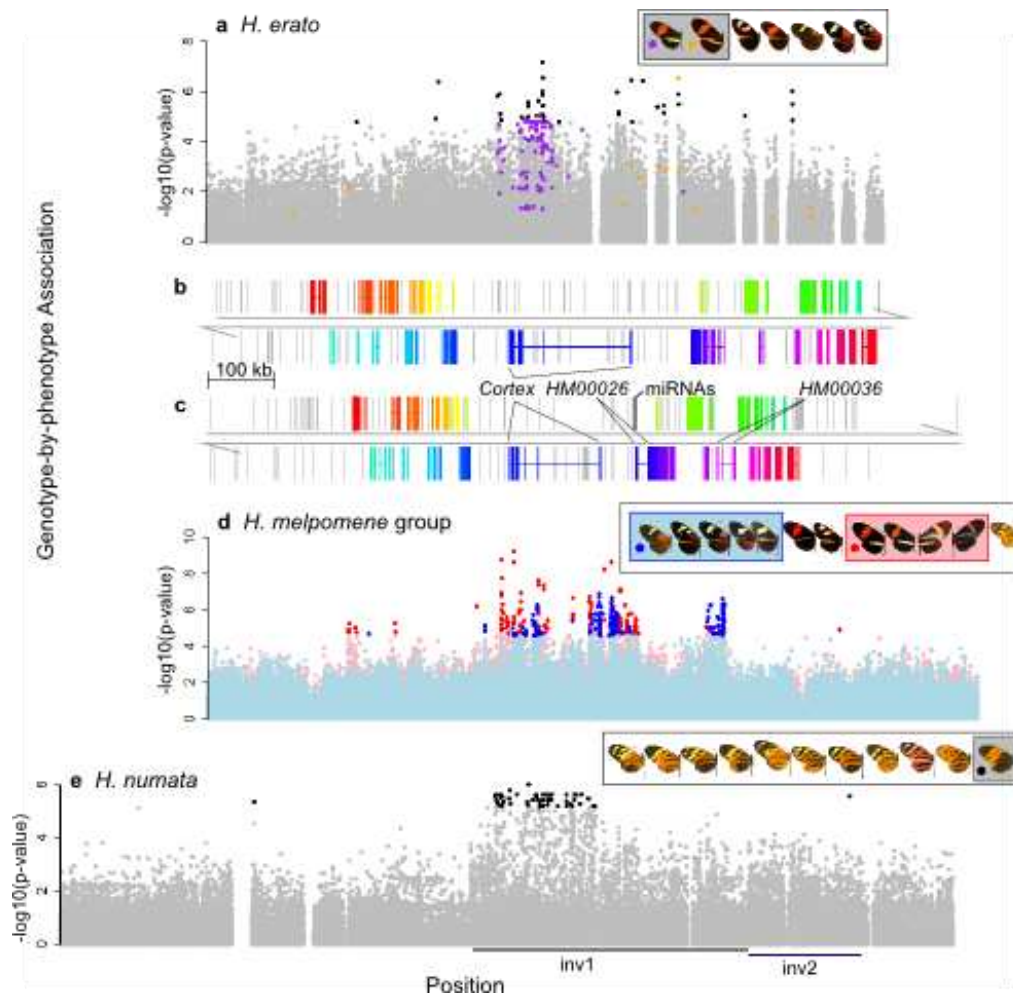
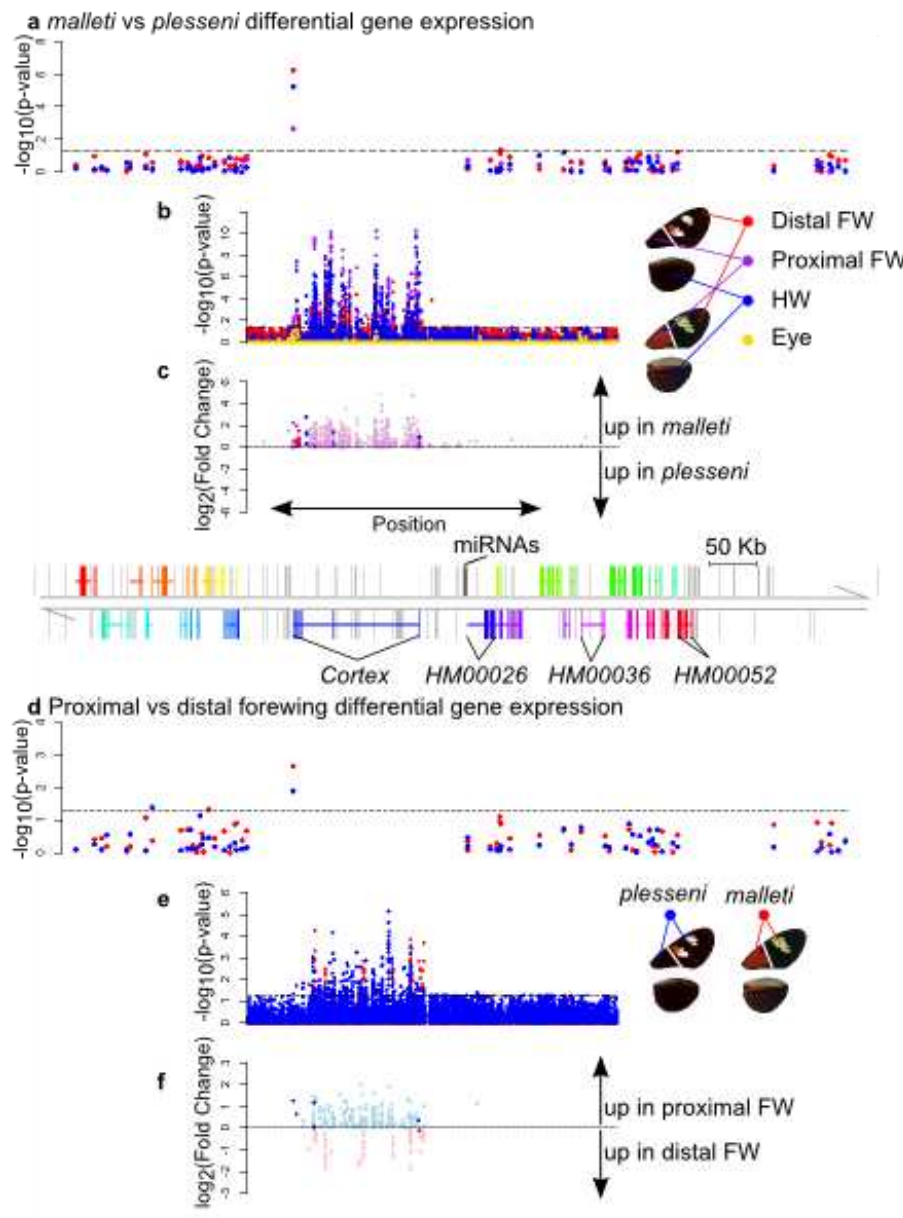


Figure 2. Association analyses across the genomic region known to contain major colour pattern loci in *Heliconius*. A) Association in He with the yellow hind-wing bar (n=45). Coloured SNPs are fixed for a unique state in He demophaon (orange) or He favorinus (purple). B) Genes in He with direct homologs in Hm. Genes are in different colours with exons (coding and UTRs) connected by a line. Grey bars are transposable elements. C) Hm genes and transposable elements: colours correspond to homologous He genes; MicroRNAs³⁰ in black. D) Association in the Hm/timareta/silvaniform group with the yellow hind-wing bar (red) and yellow forewing band (blue) (n=49). E) Association in Hn with the bicoloratus morph (n=26); inversion positions¹³ shown below. In all cases black/dark coloured points are above the strongest associations found outside the colour pattern scaffolds (He $p=1.63e-05$; Hm $p=2.03e-05$ and $p=2.58e-05$; Hn $p=6.81e-06$).



286

287 Figure 3. Differential gene expression across the genomic region known to contain major
 288 colour pattern loci in *Heliconius melpomene*. Expression differences in day 3 pupae, for all
 289 genes in the Yb interval (A,D) and tiling probes spanning the central portion of the interval
 290 (B,C,E,F). Expression is compared between races for each wing region (A,B,C) and between
 291 proximal and distal forewing sections for each race (D,E,F). C and F: magnitude and
 292 direction of expression difference (\log_2 fold-change) for tiling probes showing significant
 293 differences ($p \leq 0.05$); probes in known cortex exons shown in dark colours. Gene HM00052

was differentially expressed between other races in RNA sequence data (Supplementary Information) but is not differentially expressed here.

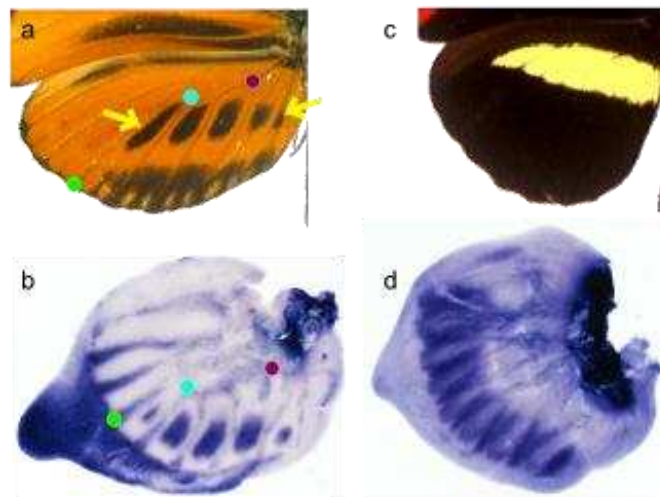


Figure 4. In situ hybridisations of cortex in hind-wings of final instar larvae. B) *Hn tarapotensis*; adult wing shown in A, coloured points indicate landmarks, yellow arrows highlight adult pattern elements corresponding to the cortex staining. D) *Hm rosina*; adult wing shown in C, staining patterns in other *Hm* races (*meriana* and *aglaope*) appeared similar. The probe used was complementary to the cortex isoform with the longest open reading frame (also the most common, Supplementary Information).

Methods

He Cr reference

Cr is the homologue of Yb in He (Fig 1). An existing reference for this region was available in 3 pieces (467,734bp, 114,741bp and 161,149bp, GenBank: KC469893.1)³¹. We screened the same BAC library used previously^{11,31} using described procedures¹¹ with probes designed

to the ends of the existing BAC sequences and the HmYb BAC reference sequence. Two BACs (04B01 and 10B14) were identified as spanning one of the gaps and sequenced using Illumina 2x250 bp paired-end reads collected on the Illumina MiSeq. The raw reads were screened to remove vector and *E. coli* bases. The first 50k read pairs were taken for each BAC and assembled individually with the Phrap³² software and manually edited with consed³³. Contigs with discordant read pairs were manually broken and properly merged using concordant read data. Gaps between contig ends were filled using an in-house finishing technique where the terminal 200bp of the contig ends were extracted and queried against the unused read data for spanning pairs, which were added using the addSolexaReads.perl script in the consed package. Finally, a single reference contig was generated by identifying and merging overlapping regions of the two consensus BAC sequences.

In order to fill the remaining gap (between positions 800,387 and 848,446) we used the overhanging ends to search the scaffolds from a preliminary He genome assembly of five Illumina paired end libraries with different insert sizes (250, 500, 800, 4300 and 6500bp) from two related He demophon individuals. We identified two scaffolds (scf1869 and scf1510) that overlapped and spanned the gap (using 12,257bp of the first scaffold and 35,803bp of the second).

The final contig was 1,009,595bp in length of which 2,281bp were unknown (N's). The HeCr assembly was verified by aligning to the HmYb genome scaffold (HE667780) with mummer and blast. The HeCr contig was annotated as described previously³², with some minor modifications. Briefly this involved first generating a reference based transcriptome assembly with existing *H. erato* RNA-seq wing tissue (GenBank accession SRA060220). We used Trimmomatic³⁴ (v0.22), and FLASH³⁵ (v1.2.2) to prepare the raw sequencing reads, checking the quality with FastQC³⁶ (v0.10.0). We then used the Bowtie/TopHat/Cufflinks³⁷⁻³⁹ pipeline

to generate transcripts for the unmasked reference sequence. We generated gene predictions with the MAKER pipeline⁴⁰ (v2.31). Homology and synteny in gene content with the Hm Yb reference were identified by aligning the Hm coding sequences to the He reference with BLAST. Homologous genes were present in the same order and orientation in He and Hm (Fig 2B,C). Annotations were manually adjusted if genes had clearly been merged or split in comparison to *H. melpomene* (which has been extensively manually curated¹²). In addition He cortex was manually curated from the RNA-seq data and using Exonerate⁴¹ alignments of the *H. melpomene* protein and mRNA transcripts, including the 5' UTRs.

Genotype-by-phenotype association analyses

Information on the individuals used and ENA accessions for sequence data are given in Supplementary Table 1. We used shotgun Illumina sequence reads from 45 He individuals from 7 races that were generated as part of a previous study³¹ (Supplementary Information). Reads were aligned to an He reference containing the Cr contig and other sequenced He BACs^{11,31} with BWA⁴², which has previously been found to work better than Stampy⁴³ (which was used for the alignments in the other species) with an incomplete reference sequence³¹. The parameters used were as follows: Maximum edit distance (n), 8; maximum number of gap opens (o), 2; maximum number of gap extensions (e), 3; seed (l), 35; maximum edit distance in seed (k), 2. We then used Picard tools to remove PCR and optical duplicate sequence reads and GATK⁴⁴ to re-align indels and call SNPs using all individuals as a single population. Expected heterozygosity was set to 0.2 in GATK. 132,397 SNPs were present across Cr. A further 52,698 SNPs not linked to colour pattern loci were used to establish background association levels.

For the Hm / Hn clade we used previously published sequence data from 19 individuals from enrichment sequencing targeting of the Yb region, the unlinked HmB/D region that controls

the presence/absence of red colour pattern elements, and ~1.8Mb of non-colour pattern genomic regions⁴⁵, as well as 9 whole genome shotgun sequenced individuals^{18,46}. We added targeted sequencing and shotgun whole genome sequencing of an additional 47 individuals (Supplementary Information). Alignments were performed using Stampy⁴³ with default parameters except for substitution rate which was set to 0.01. We again removed duplicates and used GATK to re-align indels and call SNPs with expected heterozygosity set to 0.1.

The analysis of the Hm/timareta/silvaniform included 49 individuals, which were aligned to v1.1 of the Hm reference genome with the scaffolds containing Yb and HmB/D swapped with reference BAC sequences¹⁸, which contained fewer gaps of unknown sequence than the genome scaffolds. 232,631 SNPs were present in the Yb region and a further 370,079 SNPs were used to establish background association levels.

The Hn analysis included 26 individuals aligned to unaltered v1.1 of the Hm reference genome, because the genome scaffold containing Yb is longer than the BAC reference making it easier to compare the inverted and non-inverted regions present in this species. We tested for associations at 262,137 SNPs on the Yb scaffold with the Hn bicoloratus morph, which had a sample of 5 individuals.

We measured associations between genotype and phenotype using a score test (qtscore) in the GenABEL package in R⁴⁷. This was corrected for background population structure using a test specific inflation factor, λ , calculated from the SNPs unlinked to the major colour pattern controlling loci (described above), as the colour pattern loci are known to have different population structure to the rest of the genome^{14,15,18}. We used a custom perl script to convert GATK vcf files to Illumina SNP format for input to genABEL⁴⁷. genABEL does not accept multiallelic sites, so the script also converted the genotype of any individuals for which a third (or fourth) allele was present to a missing genotype (with these defined as the lowest

frequency alleles). Custom R scripts were used to identify sites showing perfect associations with calls for >75% of individuals.

Microarray Gene Expression Analyses

We designed a Roche NimbleGen microarray (12x135K format) with probes for all annotated Hm genes¹⁸ and tiling the central portion of the Yb BAC sequence contig that was previously identified as showing the strongest differentiation between Hm races⁴⁵. In addition to the HmYb tiling array probes there were 6,560 probes tiling HmAc (a third unlinked colour pattern locus) and 10,716 probes tiling HmB/D, again distanced on average at 10bp intervals. The whole-genome gene expression array contained 107,898 probes in total.

This was interrogated with Cy3 labelled double stranded cDNA generated from total RNA (with a SuperScript double-stranded cDNA synthesis kit, Invitrogen, and a one-colour DNA labelling kit, Niblegen) from four pupal developmental stages of Hm plesseni and malleti. Pupae were from captive stocks maintained in insectary facilities in Gamboa, Panama. Tissue was stored in RNA later at -80°C prior to RNA extraction. RNA was extracted using TRIzol (Invitrogen) followed by purification with RNeasy (Qiagen) and DNase treated with DNA-free (Ambion). Quantification was performed using a Qubit 2.0 fluorometer (Invitrogen) and purity and integrity assessed using a Bioanalyzer 2100 (Agilent). Samples were randomised and each hybridised to a separate array. The HmYb probe array contained 9,979 probes distanced on average at 10bp. The whole-genome expression array contained on average 9 probes per annotated gene in the genome (v1.1¹⁸) as well as any transcripts not annotated but predicted from RNA-seq evidence.

Background corrected expression values for each probe were extracted using NimbleScan software (version 2.3). Analyses were performed with the LIMMA package implemented in R/Bioconductor⁴⁸. The tiling array and whole-genome data sets were analysed separately.

Expression values were extracted and quantile-normalised, log₂-transformed, quality controlled and analysed for differences in expression between individuals and wing regions. P-values were adjusted for multiple hypotheses testing using the False Discovery Rate (FDR) method⁴⁹.

We detected isoform-specific expression differences between Hm aglaope/amaryllis and Hm rosina/melpomene using RT-PCR and qRT-PCR on RNA extracted from developing hind-wing tissue (further details in Supplementary Information). Previously published RNAseq data was also used to assess gene expression differences between Hm aglaope and amaryllis¹⁸ (further details in Supplementary Information).

In situ hybridisations

Hn and Hm larvae were reared in a greenhouse at 25-30°C and sampled at the last instar. In situ hybridizations were performed according to previously described methods²⁵ with a cortex riboprobe synthesized from a 831-bp cDNA amplicon from Hn. Wing discs were incubated in a standard hybridization buffer containing the probe for 20-24 h at 60°C. For secondary detection of the probe, wing discs were incubated in a 1:3000 dilution of anti-digoxigenin alkaline phosphatase Fab fragments and stained with BM Purple for 3-6 h at room temperature. Stained wing discs were photographed with a Leica DFC420 digital camera mounted on a Leica Z6 APO stereomicroscope.

De novo assembly of short read data in Hm and related taxa

In order to better characterise indel variation from the short-read sequence data used for the genotype-by-phenotype association analysis, we performed de novo assemblies of a subset of Hm individuals and related taxa with a diversity of phenotypes (Extended Data Figure 2). Assemblies were performed using the de novo assembly function of CLCGenomics Workbench v.6.0 under default parameters. The assembled contigs were then BLASTed

against the Yb region of the Hm melpomene genome¹⁸, using Geneious v.8.0. The contigs identified by BLAST were then concatenated to generate an allele sequence for each individual. Occasionally two unphased alleles were generated when two contigs were matched to a given region. If more than two contigs of equal length matched then this was considered an unresolvable repeat region and replaced with Ns. The assembled alleles were then aligned using the MAFFT alignment plugin in Geneious v.8.0.

Long-range PCR targeted sequencing of cortex in Hm aglaope and Hm amaryllis

We generated two long-range PCR products covering 88.8% of the 1,344bp coding region of cortex (excluding 67bp at the 5' end and 83bp at the 3' end, further details in Supplementary Information). A product spanning coding exons 5 to 9 (the final exon) was obtained from 29 Hm amaryllis individuals and 29 Hm aglaope individuals; a product spanning coding exons 2 to 5 was obtained from 32 Hm amaryllis individuals and 14 Hm aglaope. In addition, a product spanning exons 4 to 6 was obtained from 6 Hm amaryllis and 5 Hm aglaope that failed to amplify one or both of the larger products. Long-range PCR was performed using Extensor long-range PCR mastermix (Thermo Scientific) following manufacturers guidelines with a 60°C annealing temperature in a 10-20µl volume. The product spanning coding exons 5 to 9 was obtained with primers HM25_long_F1 and HM25_long_R4 (see Supplementary Table 2 for primer sequences); the product spanning coding exons 2 to 5 was obtained with primers HM25_long_F4 and HM25_long_R2; the product spanning exons 4 to 6 was obtained with primers 25_ex5-ex7_r1 and 25_ex5-ex7_f1. Products were pooled for each individual, including 5 additional products from the Yb locus and 7 products in the region of the HmB/D locus. They were then cleaned using QIAquick PCR purification kit (QIAGEN) before being quantified with a Qubit Fluorometer (Life Technologies) and pooled in equimolar amounts for each individual, taking into account variation in the length and number of PCR products included for each individual (because of some PCR failures, ie.

proportionally less DNA was included if some PCR products were absent for a given individual).

Products were pooled within individuals (including additional products for other genes not analysed here) and then quantified and pooled in equimolar amounts for each individual within each race. The pooled products for each race (Hm aglaope and amaryllis) were then prepared as two separate libraries with molecular identifiers and sequenced on a single lane of an Illumina GAIIx. Analysis was performed using Galaxy and the history is available at <https://usegalaxy.org/u/njnadeau/h/long-pcr-final>. Reads were quality filtered with a minimum quality of 20 required over 90% of the read, which resulted in 5% of reads being discarded. Reads were then quality trimmed to remove bases with quality less than 20 from the ends. They were then aligned to the target regions using the fosmid sequences from known races⁴⁵ with sequence from the Yb BAC walk¹² used to fill any gaps. Alignments were performed with BWA v0.5.6⁴² and converted to pileup format using Samtools v0.1.12 before being filtered based on quality (≥ 20) and coverage (≥ 10). BWA alignment parameters were as follows: fraction of missing alignments given 2% uniform base error rate (aln -n) 0.01; maximum number of gap opens (aln -o) 2; maximum number of gap extensions (aln -e) 12; disallow long deletion within 12 bp towards the 3'-end (aln -d); number of first subsequences to take as seed (aln -l) 100. We then calculated coverage and minor allele frequencies for each race and the difference between these using custom scripts in R⁵⁰.

Sequencing and analysis of Hm fosmid clones

Fosmid libraries had previously been made from single individuals of 3 Hm races (rosina, amaryllis and aglaope) and several clones overlapping the Yb interval had been sequenced⁴⁵. We extended the sequencing of this region, particularly the region overlapping cortex by sequencing an additional 4 clones from Hm rosina (1051_83D21, accession KU514430;

1051_97A3, accession KU514431; 1051_65N6, accession KU514432; 1051_93D23, accession KU514433) 2 clones from Hm amaryllis (1051_13K4, accession KU514434; 1049_8P23, accession KU514435) and 3 clones from Hm aglaope (1048_80B22, accession KU514437; 1049_19P15, accession KU514436; 1048_96A7, accession KU514438). These were sequenced on a MiSeq 2000, and assembled using the de novo assembly function of CLC Genomics Workbench v.6.0. The individual clones (including existing clones 1051-143B3, accession FP578990; 1049-27G11, accession FP700055; 1048-62H20, accession FP565804) were then aligned to the BAC and genome scaffold¹⁸ references using the MAFFT alignment plugin of Geneious v.8.0. Regions of general sequence similarity were identified and visualised using MAUVE⁵¹. We merged overlapping clones from the same individual if they showed no sequence differences, indicating that they came from the same allele. We identified transposable elements (TEs) using nBLAST with an insect TE list downloaded from Repbase Update⁵² including known *Heliconius* specific TEs⁵³.

5' RACE, RT-PCR and qRT-PCR

All tissues used for gene expression analyses were dissected from individuals from captive stocks derived from wild caught individuals of various races of Hm (aglaope, amaryllis, melpomene, rosina, plesseni, malleti) and F2 individuals from a Hm rosina (female) x Hm melpomene (male) cross. Experimental individuals were reared at 28°C-31°C. Developing wings were dissected and stored in RNAlater (Ambion Life Technologies). RNA was extracted using a QIAgen RNeasy Mini kit following the manufacturer's guidelines and treated with TURBO DNA-free DNase kit (Ambion Life Technologies) to remove remaining genomic DNA. RNA quantification was performed with a Nanodrop spectrophotometer, and the RNA integrity was assessed using the Bioanalyzer 2100 system (Agilent).

503 Total RNA was thoroughly checked for DNA contamination by performing PCR for EF1 α
 504 (using primers ef1-a_RT_for and ef1-a_RT_rev, Table S2) with 0.5 μ l of RNA extract (50ng-
 505 1 μ g of RNA) in a 20 μ l reaction using a polymerase enzyme that is not functional with RNA
 506 template (BioScript, Bioline Reagents Ltd.). If a product amplified within 45 cycles then the
 507 RNA sample was re-treated with DNase.

508 Single stranded cDNA was synthesised using BioScript MMLV Reverse Transcriptase
 509 (Bioline Reagents Ltd.) with random hexamer (N6) primers and 1 μ g of template RNA from
 510 each sample in a 20 μ l reaction volume following the manufacturer's protocol. The resulting
 511 cDNA samples were then diluted 1:1 with nuclease free water and stored at -80°C.

512 5' RACE was performed using RNA from hind-wing discs from one Hm aglaope and one
 513 Hm amaryllis final instar larvae with a SMARTer RACE kit from Clontech (California,
 514 USA). The gene specific primer used for the first round of amplification was anchored in
 515 exon 4 (fzl_raceex5_R1, Supplementary Table 2). Secondary PCR of these products was then
 516 performed using a primer in exon 2 (HM25_long_F2, Supplementary Table 2) and the nested
 517 universal primer A. Other isoforms were detected by RT-PCR using primers within exons 2
 518 and 9 (gene25_for_full1 and gene25_rev_ex3). We identified isoforms from 5' RACE and
 519 RT-PCR products by cutting individual bands from agarose gels and if necessary by cloning
 520 products before Sanger sequencing. Cloning of products was performed using TOPO TA
 521 (Invitrogen) or pGEM-T (Promega) cloning kits. Sanger sequencing was performed using
 522 BigDye terminator v3.1 (Applied Biosystems) run on an ABI13730 capillary sequencer.
 523 Primers fzl_ex1a_F1 and fzl_ex4_R1 were used to confirm expression of the furthest 5'
 524 UTR. For isoforms that appeared to show some degree of race specificity we designed
 525 isoform specific PCR primers spanning specific exon junctions (Extended Data Fig 2, 4,
 526 Supplementary Table 2) and used these to either qualitatively (RT-PCR) or quantitatively
 527 (qRT-PCR) assess differences in expression between races.

We performed qRT-PCR using SensiMix SYBR green (Bioline Reagents Ltd.) with 0.2-0.25 μ M of each primer and 1 μ l of the diluted product from the cDNA reactions. Reactions were performed in an Opticon 2 DNA engine (MJ Research), with the following cycling parameters: 95°C for 10min, 35-50 x: (95°C for 15sec, 55-60°C for 30sec, 72° for 30sec), 72°C for 5min. Melting curves were generated between 55°C and 90°C with readings taken every 0.2°C for each of the products to check that a single product was generated. At least one product from each set of primers was also run on a 1% agarose gel to check that a single product of the expected size was produced and the identity of the product confirmed by direct sequencing (See Supplementary Table 2 for details of primers for each gene). We used two housekeeping genes (*EF1 α* and Ribosomal Protein S3A) for normalisation and all results were taken as averages of triplicate PCR reactions for each sample.

C_t values were defined as the point at which fluorescence crossed a threshold (R_{Ct}) adjusted manually to be the point at which fluorescence rose above the background level. Amplification efficiencies (E) were calculated using a dilution series of clean PCR product. Starting fluorescence, which is proportional to the starting template quantity, was calculated as $R_0 = R_{Ct} (1+E)^{-Ct}$. Normalized values were then obtained by dividing R_0 values for the target loci by R_0 values for *EF1 α* and *RPS3A*. Results from both of these controls were always very similar, therefore the results presented are normalized to the mean of *EF1 α* and *RPS3A*. All results were taken as averages of triplicate PCR reactions. If one of the triplicate values was more than one cycle away from the mean then this replicate was excluded. Similarly any individuals that were more than two standard deviations away from the mean of all individuals for the target or normalization genes were excluded (these are not included in the numbers of individuals reported). Statistical significance was assessed by Wilcoxon rank sum tests performed in R⁵⁰.

RNAseq analysis of *Hm amaryllis/aglaope*

RNA-seq data for hind-wings from three developmental stages had previously been obtained for two individuals of each race at each stage (12 individuals in total) and used in the annotation of the Hm genome¹⁸ (deposited in ENA under study accessions ERP000993 and PRJEB7951). Four samples were multiplexed on each sequencing lane with the fifth instar larval and day 2 pupal samples sequenced on a GAIIx sequencer and the day 3 pupal wings sequenced on a Hiseq 2000 sequencer.

Two methods were used for alignment of reads to the reference genome and inferring read counts, Stampy⁴³ and RSEM (RNAseq by Expectation Maximisation)⁵⁴. In addition we used two different R/Bioconductor packages for estimation of differential gene expression, DESeq⁵⁵ and BaySeq⁵⁶. Read bases with quality scores < 20 were trimmed with FASTX-Toolkit (http://hannonlab.cshl.edu/fastx_toolkit/index.html). Stampy was run with default parameters except for mean insert size, which was set to 500, SD 100 and substitution rate, which was set to 0.01. Alignments were filtered to exclude reads with mapping quality <30 and sorted using Samtools⁵⁷. We used the HT seq-count script in with HTseq⁵⁸ to infer counts per gene from the BAM files.

RSEM⁵⁴ was run with default parameters to infer a transcriptome and then map RNAseq reads against this using Bowtie³⁷ as an aligner. This was run with default parameters except maximum number of mismatches, which was set to 3.

Annotation and alignment of fizzy family proteins

In the arthropod genomes, some fizzy family proteins were found to be poorly annotated based on alignments to other family members. In these cases annotations were improved using well annotated proteins from other species as references in the program Exonerate⁴¹ and the outputs were manually curated. Specifically, the annotation of *B. mori* fzr was extended based on alignment of *D. plexippus* fzr; the annotation of *B. mori* fzy was altered

based on alignment of *Drosophila melanogaster* and *D. plexippus* fzy; *H. melpomene* fzy was identified as part of the annotated gene HMEL017486 on scaffold HE671623 (Hmel v1.1) based on alignment of *D. plexippus* fzy; the *Apis mellifera* fzf annotation was altered based on alignment of *D. melanogaster* fzf; the annotation of *Acyrtosiphon pisum* fzf was altered based on alignment of *D. melanogaster* fzf. No one-to-one orthologues of *D. melanogaster* fzf2 were found in any of the other arthropod genera, suggesting that this gene is *Drosophila* specific. Multiple sequence alignment of all the fizzy family proteins was then performed using the Expresso server⁵⁹ within T-coffee⁶⁰, and this alignment was used to generate a neighbour joining tree in Geneious v8.1.7.

Expression of *H. melpomene* cortex in *D. melanogaster* wings

D. melanogaster Cortex is known to generate an irregular microchaete phenotype when ectopically expressed in the posterior compartment of the adult fly wing²⁴. We performed the same assay using *H. melpomene* cortex in order to test if this functionality was conserved. Following the methods of Swan and Schüpbach²⁴ a UAS-GAL4 construct was created using the coding region for the long isoform of Hm cortex, plus a *Drosophila* cortex version to act as positive control. The HA-tagged *H. melpomene* UAS-cortex expression construct was generated using cDNA reverse transcribed (Revert-Aid, Thermo-Scientific) from RNA extracted (Qiagen RNeasy) from pre-ommochrome pupal wing material. An HA-tagged *D. melanogaster* UAS-cortex version was also constructed, following the methods of Swan and Schüpbach, (2007). Expression was driven by hsp70 promoter. Constructs were injected into ϕ C31-attP40 flies (#25709, Bloomington stock centre, Indiana; Cambridge University Genetics Department, UK, fly injection service) by site directed insertion into CII via an attB site in the construct. Homozygous transgenic flies were crossed with w,y';en-GAL4;UAS-GFP (gift of M. Landgraf lab, Cambridge University Zoology Department) to drive

expression in the engrailed posterior domain of the wing, and adult offspring wings photographed (Extended Data Fig 6B-D). Expression of the construct was confirmed by IHC (standard *Drosophila* protocol) of final instar larval wing discs using mouse anti-HA and goat anti-mouse alexa-fluor 568 secondary antibodies (Abcam), imaged by Leica SP5 confocal. Successful expression of Hm_Cortex was confirmed by IHC against an HA tag inserted at the N terminal of either protein (Extended Data Fig 6E).

References

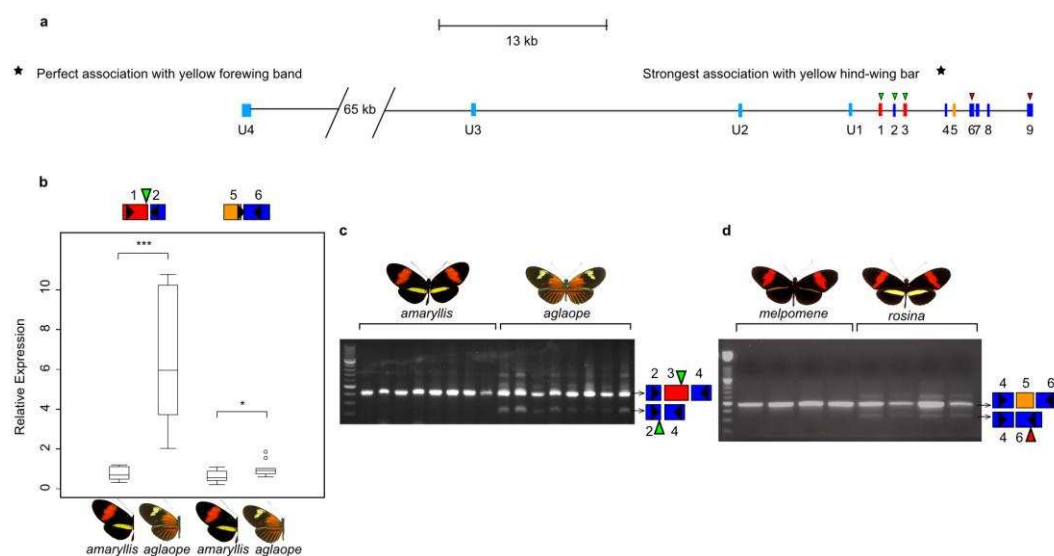
31. Supple, M. A. et al. Genomic architecture of adaptive color pattern divergence and convergence in *Heliconius* butterflies. *Genome Res.* **23**, 1248–1257 (2013).
32. de la Bastide, M. & McCombie, W. R. Assembling genomic DNA sequences with PHRAP. *Curr. Protoc. Bioinforma.* Ed. Board Andreas Baxevanis Al **Chapter 11**, Unit11.4 (2007).
33. Gordon, D., Abajian, C. & Green, P. Consed: a graphical tool for sequence finishing. *Genome Res.* **8**, 195–202 (1998).
34. Bolger, A. M., Lohse, M. & Usadel, B. Trimmomatic: a flexible trimmer for Illumina sequence data. *Bioinformatics* **btu170** (2014). doi:10.1093/bioinformatics/btu170
35. Magoč, T. & Salzberg, S. L. FLASH: fast length adjustment of short reads to improve genome assemblies. *Bioinformatics* **27**, 2957–2963 (2011).
36. Andrews, S. FastQC. (2011).
37. Langmead, B., Trapnell, C., Pop, M. & Salzberg, S. L. Ultrafast and memory-efficient alignment of short DNA sequences to the human genome. *Genome Biol.* **10**, R25 (2009).
38. Trapnell, C., Pachter, L. & Salzberg, S. L. TopHat: discovering splice junctions with RNA-Seq. *Bioinformatics* **25**, 1105–1111 (2009).

- 625 39. Trapnell, C. et al. Transcript assembly and quantification by RNA-Seq reveals
 626 unannotated transcripts and isoform switching during cell differentiation. *Nat.*
 627 *Biotechnol.* **28**, 511–515 (2010).
- 628 40. Holt, C. & Yandell, M. MAKER2: an annotation pipeline and genome-database
 629 management tool for second-generation genome projects. *BMC Bioinformatics* **12**, 491
 630 (2011).
- 631 41. Slater, G. S. & Birney, E. Automated generation of heuristics for biological sequence
 632 comparison. *BMC Bioinformatics* **6**, 31 (2005).
- 633 42. Li, H. & Durbin, R. Fast and accurate short read alignment with Burrows-Wheeler
 634 transform. *Bioinforma. Oxf. Engl.* **25**, 1754–1760 (2009).
- 635 43. Lunter, G. & Goodson, M. Stampy: A statistical algorithm for sensitive and fast mapping
 636 of Illumina sequence reads. *Genome Res.* **21**, 936–939 (2011).
- 637 44. DePristo, M. A. et al. A framework for variation discovery and genotyping using next-
 638 generation DNA sequencing data. *Nat Genet* **43**, 491–498 (2011).
- 639 45. Nadeau, N. J. et al. Genomic islands of divergence in hybridizing *Heliconius* butterflies
 640 identified by large-scale targeted sequencing. *Philos. Trans. R. Soc. B Biol. Sci.* **367**,
 641 343–353 (2012).
- 642 46. Martin, S. H. et al. Genome-wide evidence for speciation with gene flow in *Heliconius*
 643 butterflies. *Genome Res.* **23**, 1817–1828 (2013).
- 644 47. Aulchenko, Y. S., Ripke, S., Isaacs, A. & van Duijn, C. M. GenABEL: an R library for
 645 genome-wide association analysis. *Bioinforma. Oxf. Engl.* **23**, 1294–1296 (2007).
- 646 48. Smyth, G. K. in *Bioinformatics and Computational Biology Solutions Using R and*
 647 *Bioconductor* (eds. Gentleman, R., Carey, V. J., Huber, W., Irizarry, R. A. & Dudoit, S.)
 648 397–420 (Springer New York, 2005).

- 649 49. Benjamini, Y. & Hochberg, Y. Controlling the False Discovery Rate: A Practical and
 650 Powerful Approach to Multiple Testing. *J. R. Stat. Soc. Ser. B Methodol.* **57**, 289–300
 651 (1995).
- 652 50. R Development Core Team. R: A language and environment for statistical computing.
 653 (R Foundation for Statistical Computing, 2011).
- 654 51. Darling, A. C. E., Mau, B., Blattner, F. R. & Perna, N. T. Mauve: Multiple Alignment of
 655 Conserved Genomic Sequence With Rearrangements. *Genome Res.* **14**, 1394–1403
 656 (2004).
- 657 52. Jurka, J. et al. Repbase Update, a database of eukaryotic repetitive elements. *Cytogenet.*
 658 *Genome Res.* **110**, 462–467 (2005).
- 659 53. Lavoie, C. A., Platt, R. N., Novick, P. A., Counterman, B. A. & Ray, D. A. Transposable
 660 element evolution in *Heliconius* suggests genome diversity within Lepidoptera. *Mob.*
 661 *DNA* **4**, 21 (2013).
- 662 54. Li, B. & Dewey, C. N. RSEM: accurate transcript quantification from RNA-Seq data
 663 with or without a reference genome. *BMC Bioinformatics* **12**, 323 (2011).
- 664 55. Anders, S. & Huber, W. Differential expression analysis for sequence count data.
 665 *Genome Biol.* **11**, 1–12 (2010).
- 666 56. Hardcastle, T. J. & Kelly, K. A. baySeq: Empirical Bayesian methods for identifying
 667 differential expression in sequence count data. *BMC Bioinformatics* **11**, 422 (2010).
- 668 57. Li, H. et al. The Sequence Alignment/Map format and SAMtools. *Bioinforma. Oxf. Engl.*
 669 **25**, 2078–2079 (2009).
- 670 58. Anders, S., Pyl, P. T. & Huber, W. HTSeq - A Python framework to work with high-
 671 throughput sequencing data. *bioRxiv* (2014). doi:10.1101/002824

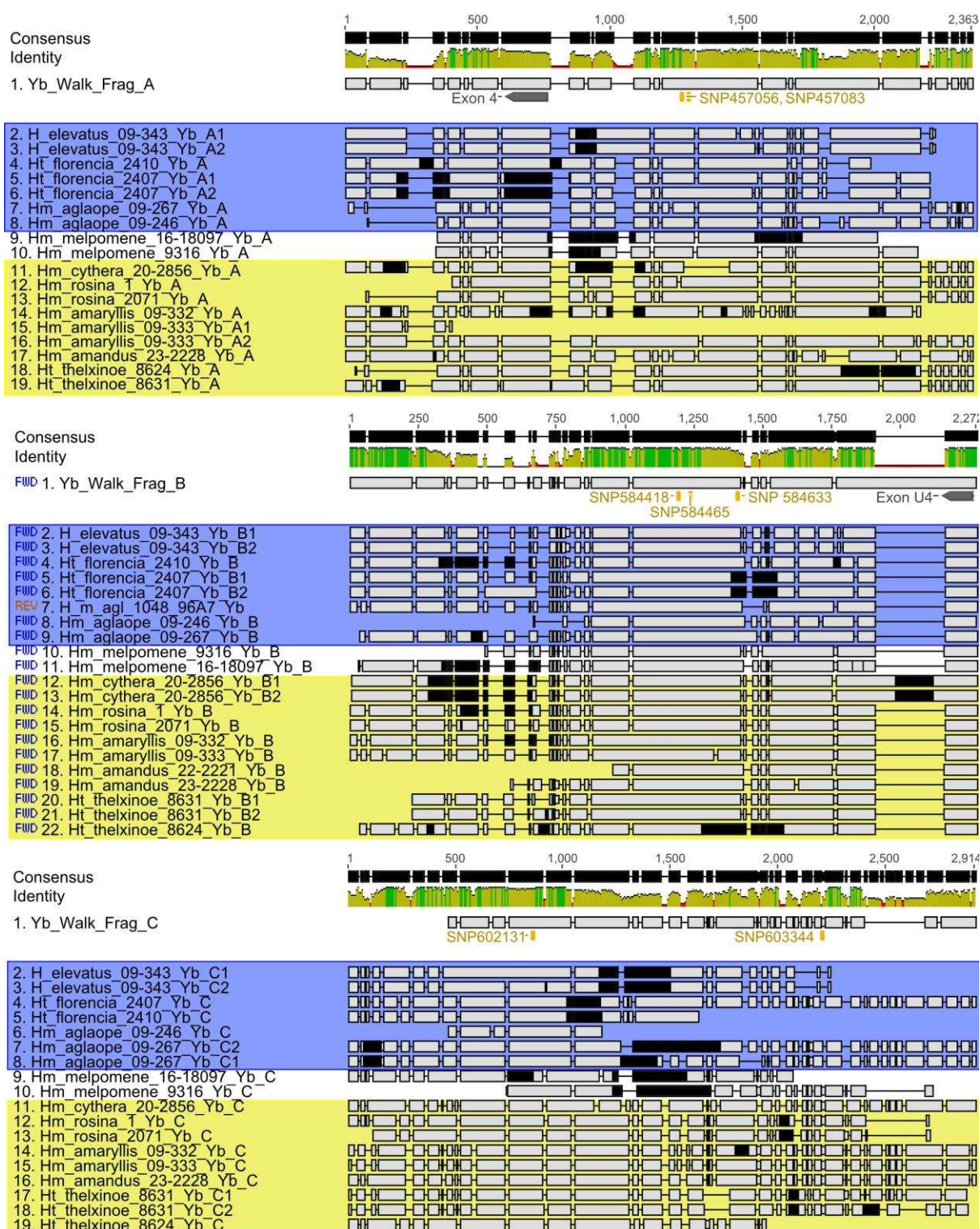
59. Armougom, F. et al. Expresso: automatic incorporation of structural information in multiple sequence alignments using 3D-Coffee. *Nucleic Acids Res.* **34**, W604–608 (2006).
60. Di Tommaso, P. et al. T-Coffee: a web server for the multiple sequence alignment of protein and RNA sequences using structural information and homology extension. *Nucleic Acids Res.* **39**, W13–17 (2011).

Extended Data



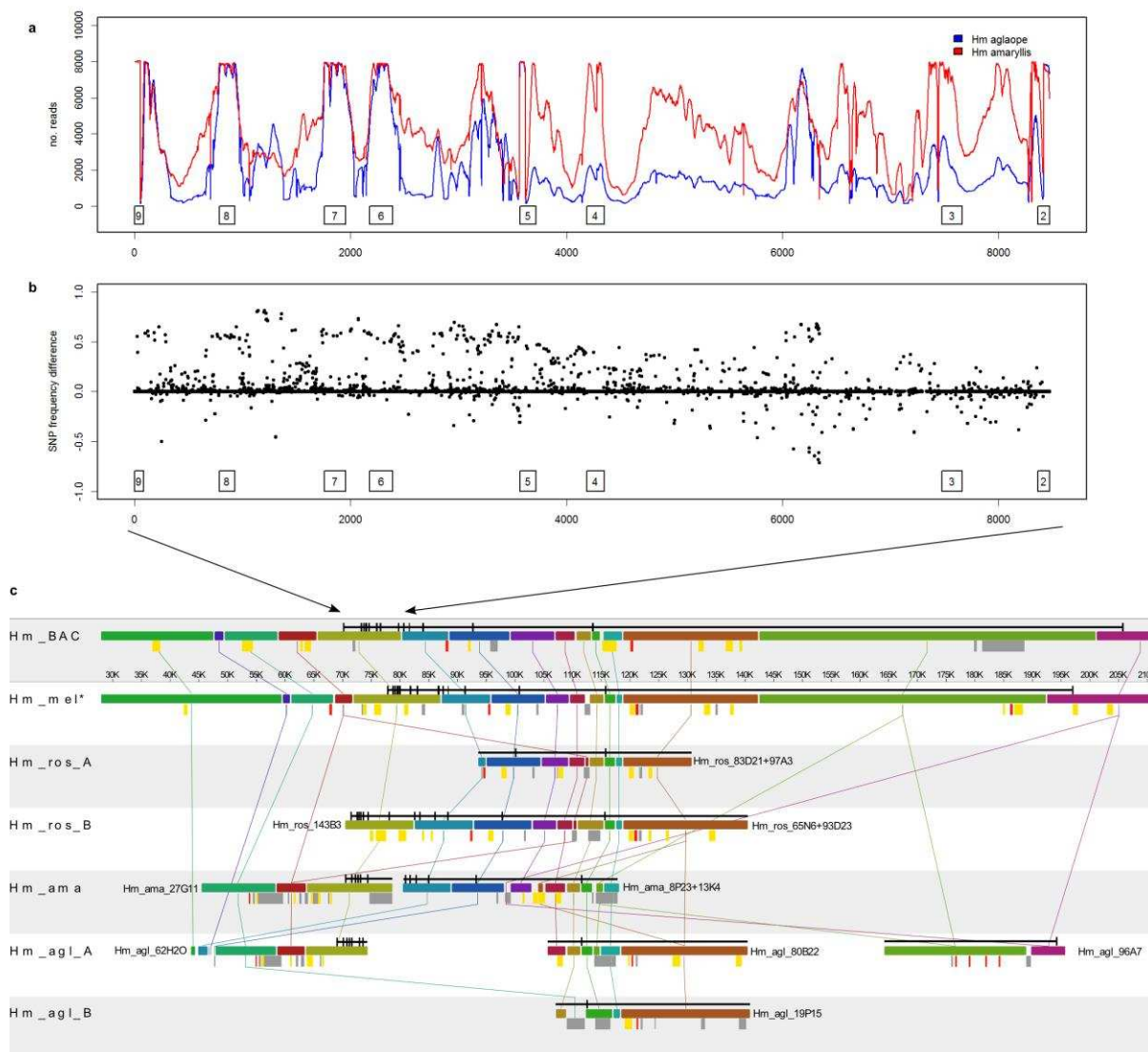
Extended Data Figure 1. A) Exons and splice variants of cortex in Hm. Orientation is reversed with respect to figures 2 and 4, with transcription going from left to right. SNPs showing the strongest associations with phenotype are shown with stars. B) Differential expression of two regions of cortex between Hm amaryllis and Hm aglaope whole hindwings (N=11 and N=10 respectively). Boxplots are standard (median; 75th and 25th percentiles; maximum and minimum excluding outliers – shown as discrete points) C) Expression of a

688 cortex isoform lacking exon 3 is found in Hm aglaope but not Hm amaryllis hindwings. D)
689 Expression of an isoform lacking exon 5 is found in Hm rosina but not Hm melpomene
690 hindwings. Green triangles indicate predicted start codons and red triangles predicted stop
691 codons, with usage dependent on which exons are present in the isoform. Schematics of the
692 targeted exons are shown for each (q)RT-PCR product, black triangles indicate the position
693 of the primers used in the assay.



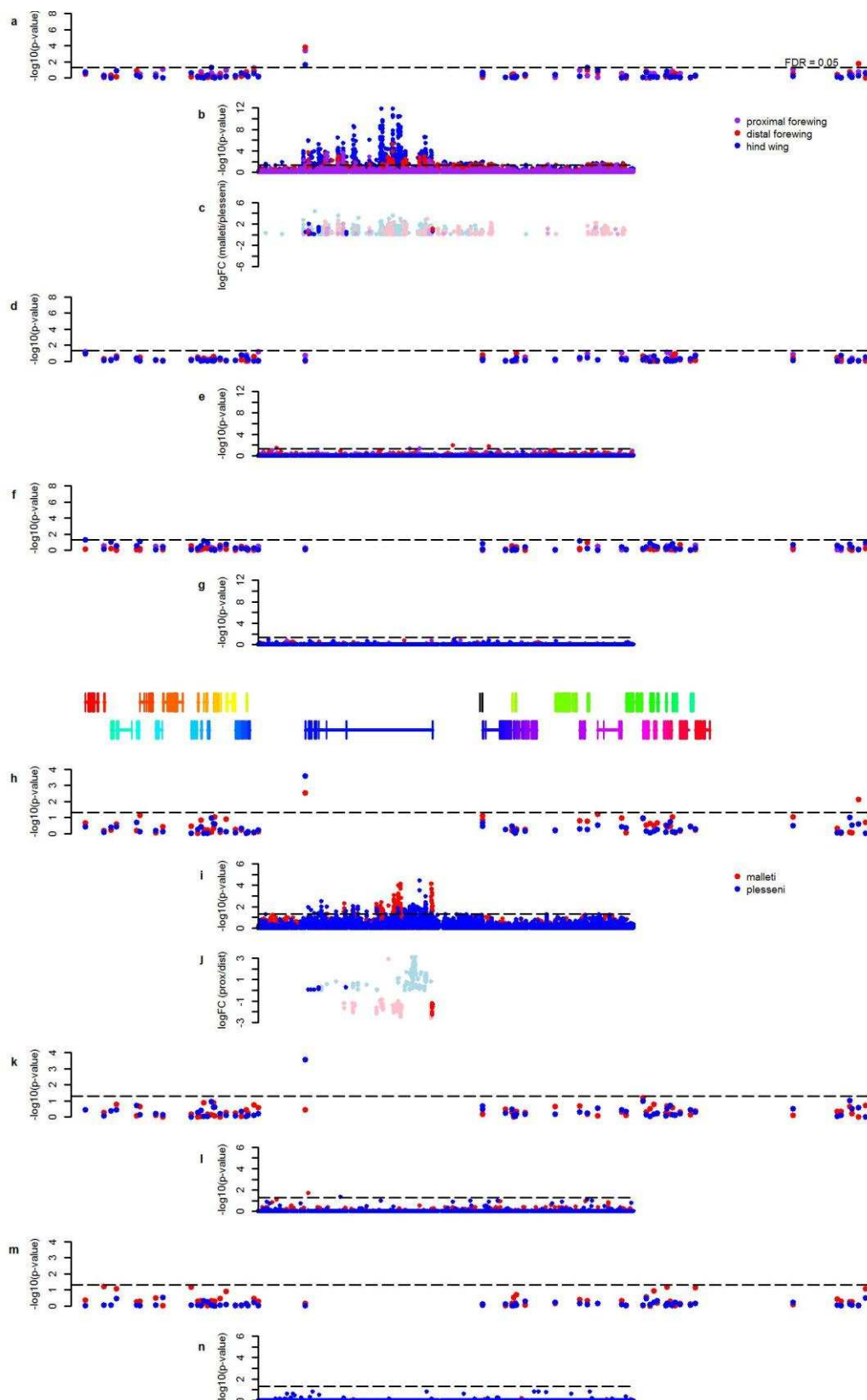
Extended Data Figure 2. Alignments of de novo assembled fragments containing the top associated SNPs from Hm and related taxa short-read data. Identified indels do not show stronger associations with phenotype than those seen at SNPs (as shown in Extended Data Table 2), although some near-perfect associations are seen in fragment C. Black regions =

699 missing data; yellow box = individuals with a hindwing yellow bar; blue box = individuals
 700 with a yellow forewing band.



701
 702 Extended Data Figure 3. Sequencing of long-range PCR products and fosmids spanning
 703 cortex. A) Sequence read coverage from long-range PCR products across the cortex coding
 704 region from 2 Hm races. B) Minor allele frequency difference from these reads between Hm
 705 aglaope and Hm amaryllis. Exons of cortex are indicated by boxes, numbered as in Extended
 706 Data Figure 2. C) Alignments of sequenced fosmids overlapping cortex from 3 Hm
 707 individuals of difference races. No major rearrangements are observed, nor any major
 708 differences in transposable element (TE) content between closely related races with different

709 colour patterns (melpomene/rosina or amaryllis/aglaope). Hm amaryllis and rosina have the
710 same phenotype, but do not share any TEs that are not present in the other races. Hm_BAC =
711 BAC reference sequence, Hm_mel = melpomene from new unpublished assembly of Hm
712 genome⁵¹, Hm_ros = rosina (2 different alleles were sequenced from this individual),
713 Hm_ama = amaryllis (2 non-overlapping clones were sequenced in this individual), Hm_agla
714 = aglaope (4 clones were sequenced in this individual 2 of which represent alternative
715 alleles). Alignments were performed with Mauve: coloured bars represent homologous
716 genomic regions. cortex is annotated in black above each clone. Variable TEs are shown as
717 coloured bars below each clone: red = Metulj-like non-LTR, yellow = Helitron-like DNA,
718 grey = other.

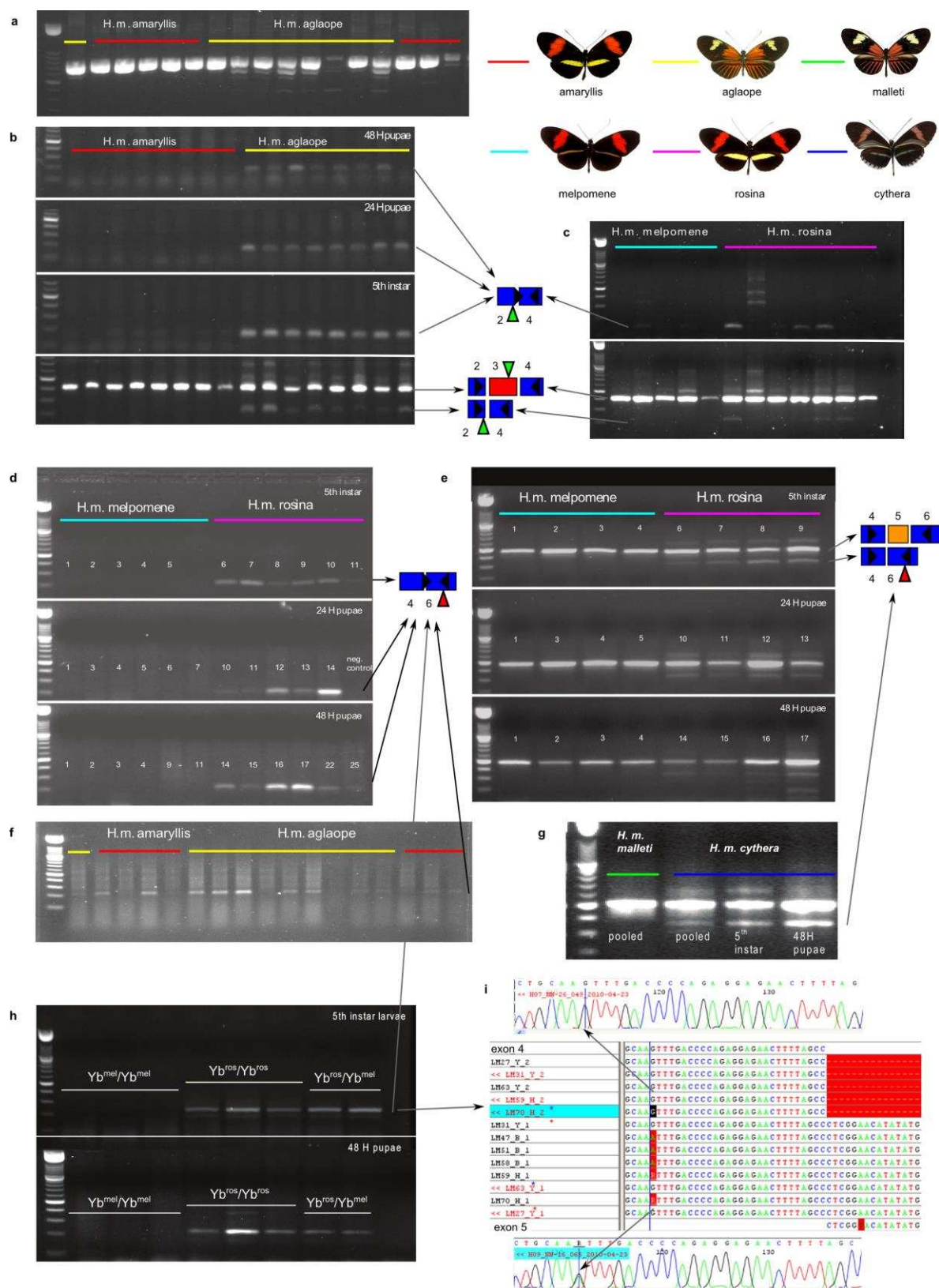


719

720 Extended Data Figure 4. Expression array results for additional stages, related to Figure 4. A-

721 G: comparisons between races (H. m. plesseni and H. m. malleti) for 3 wing regions. H-N:

722 comparisons between proximal and distal forewing regions for each race. Significance values
723 ($-\log_{10}(\text{p-value})$) are shown separately for genes in the HmYb region from the gene array
724 (A,D,F,H,K,M) and for the HmYb tiling array (B,E,G,I,L,N) for day 1 (A,B,H,I), day 5
725 (D,E,K,L) and day 7 (F,G,M,N) after pupation. The level of expression difference (log fold
726 change) for tiling probes showing significant differences ($p \leq 0.05$) is shown for day 1 (C and
727 J) with probes in known cortex exons shown in dark colours and probes elsewhere shown as
728 pale colours.

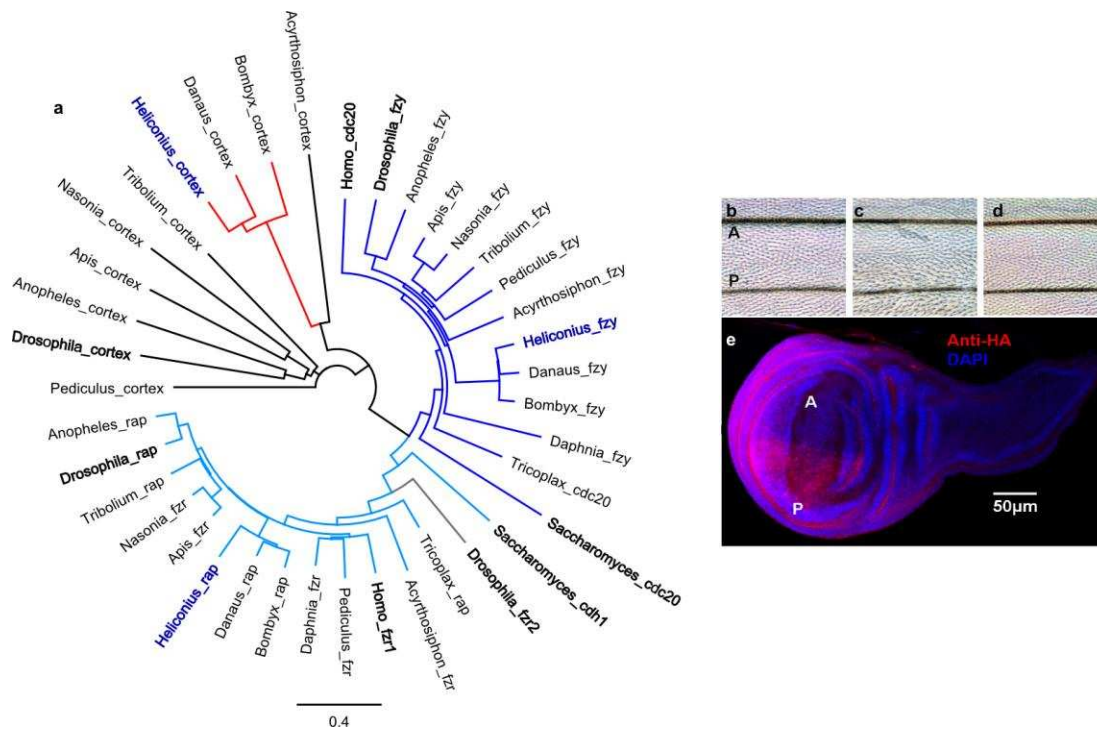


729

730 Extended Data Figure 5. Alternative splicing of cortex. A) Amplification of the whole cortex

731 coding region, showing the diversity of isoforms and variation between individuals. B)

732 Differences in splicing of exon 3 between *H. m. aglaope* and *H. m. amaryllis*. Products
 733 amplified with a primer spanning the exon 2/4 junction at 3 developmental stages. The lower
 734 panel shows verification of this assay by amplification between exons 2 and 4 for the same
 735 final instar larval samples (replicated in Extended Data Figure 2C) C) Lack of consistent
 736 differences between *H. m. melpomene* and *H. m. rosina* in splicing of exon 3. Top panel
 737 shows products amplified with a primer spanning the exon 2/4 junction, lower panel is the
 738 same samples amplified between exons 2 and 4. D) Differences in splicing of exon 5 between
 739 *H. m. melpomene* and *H. m. rosina*. Products amplified with a primer spanning the exon 4/6
 740 junction at 3 developmental stages. E) Subset of samples from D amplified with primers
 741 between exons 4 and 6 for verification (middle, 24hr pupae samples are replicated in
 742 Extended Data Figure 2D). F) Lack of consistent differences between *H. m. aglaope* and *H.*
 743 *m. amaryllis* in splicing of exon 5. Products amplified with a primer spanning the exon 4/6
 744 junction. G) *H. m. cythera* also expresses the isoform lacking exon 5, while a pool of 6 *H. m.*
 745 *malleti* individuals do not. H) Expression of the isoform lacking exon 5 from an F2 *H. m.*
 746 *melpomene* x *H. m. rosina* cross. Individuals homozygous or heterozygous for the *H. m.*
 747 *rosina* HmYb allele express the isoform while those homozygous for the *H. m. melpomene*
 748 HmYb allele do not. I) Allele specific expression of isoforms with and without exon 5.
 749 Heterozygous individuals (indicated with blue and red stars) express only the *H. m. rosina*
 750 allele in the isoform lacking exon 5 (G at highlighted position), while they express both
 751 alleles in the isoform containing exon 5 (G/A at this position).



Extended Data Figure 6. Phylogeny of fizzy family proteins and effects of expressing cortex in the *Drosophila* wing. A) Neighbour joining phylogeny of Fizzy family proteins including functionally characterised proteins (in bold) from *Saccharomyces cerevisiae*, *Homo sapiens* and *Drosophila melanogaster* as well as copies from the basal metazoan *Trichoplax adhaerens* and a range of annotated arthropod genomes (*Daphnia pulex*, *Acyrthosiphon pisum*, *Pediculus humanus*, *Apis mellifica*, *Nasonia vitripennis*, *Anopheles gambiae*, *Tribolium castaneum*) including the lepidoptera *H. melpomene* (in blue), *Danaus plexippus* and *Bombyx mori*. Branch colours: dark blue, CDC20/fzy; light blue, CDH1/fzr/rap; red, lepidopteran cortex. B-E) Ectopic expression of cortex in *Drosophila melanogaster*. *Drosophila cortex* produces an irregular microchaete phenotype when expressed in the posterior compartment of the fly wing (C) whereas *Heliconius cortex* does not (D), when compared to no expression (B). A, anterior; P, posterior. Successful *Heliconius cortex* expression was confirmed by anti-HA IHC in the last instar *Drosophila* larva wing imaginal disc (D, red), with DAPI staining in blue.

767 Extended Data Table 1. Genes in the Yb region and evidence for wing patterning control in
 768 *Heliconius*

<i>Hm</i> gene ID	<i>He</i> gene ID	Putative gene name	<i>Heliconius melpomene</i>										<i>H. erato</i>			<i>Hn</i>	
			Yb ^l	Sb ^l	A ^{Yb}	A ^N	E ¹	E ^{9w}	E ^{9r}	E ^{hw}	E ^{tr}	Cr ^l	A ^{pot}	A ^{fav}	P ^l	A ^{bic}	
HM00002	HERA000036	Acylpeptide hydrolase			2							x					
HM00003	HERA000037	HM00003										x					
HM00004	HERA000038	Trehalase-1B	x									x					
HM00006	HERA000038.1	Trehalase-1A	x									x					
HM00007	HERA000039	B9 protein	x									x					
HM00008	HERA000040	HM00008	x		2							x					
HM00010	HERA000041	WD40 repeat domain 85	x									x					
HM00012	HERA000042	CG2519	x					x				x					
HM00013	HERA000045	Unkempt	x									x					
HM00014	HERA000046	Histone H3	x									x					
HM00015	HERA000047	HM00015	x									x					
HM00016	HERA000048	HM00016	x									x					
HM00017	HERA000049	RecQ Helicase	x									x					
HM00018	HERA000051	HM00018	x									x					
HM00019	HERA000052	BmSuc2	x					x				x					
HM00020	HERA000053	CG5796	x									x					
HM00021	HERA000054	HM00021	x									x					
HM00022	HERA000055	Enoyl-CoA hydratase	x									x					
HM00023	HERA000056	ATP binding protein	x									x					
HM00024	HERA000057	HM00024	x									x					
HM00025	HERA000059	cortex	x	x	56	74	x	x	x	603	1796	x	2	99	x	51	
HM00026	HERA000077	Poly(A)-specific ribonuclease (pam)		x	10					1	34	x				x	
HM00027	HERA000079	CG31320		x								x				x	
HM00028	HERA000080	ARP-like		x								x				x	
HM00029	HERA000081	CG4692		x								x				x	
HM00030	HERA000082	Proteasome 26S non ATPase subunit 4		x								x				x	
HM00031	HERA000083	HM00031		x					x			x				x	
HM00032	HERA000084	Zinc phosphodiesterase		x							1	x				x	
HM00033	HERA000085	Serine/threonine-protein kinase (LMTK1)		x							8	x				x	
HM00034	HERA000086	WD repeat domain 13 (Wdr13)			1	4					5	x				x	
HM00035	HERA000087	Domeless			1	2						x				x	
HM00036	HERA000061	WAS protein family homologue 1			5	36					37	x				x	
HM00038	HERA000062	Lethal (2) k05819 CG3054										x	2			x	
HM00039	HERA000064	Mitogen-activated protein kinase (MAPKK)										x				x	
HM00040	HERA000064.1	DNA excision repair protein ERCC-6										x				x	
HM00041	HERA000065	Penguin										x				x	
HM00042	HERA000066	Thymidylate kinase										x				x	
HM00043	HERA000067	Caspase-activated DNase										x				x	
HM00044	HERA000068	Regulator of ribosome biosynthesis										x				x	
HM00045	HERA000069	CG12659										x				x	
HM00046	HERA000070	CG33505										x				x	
HM00047	HERA000071	Sr protein										x				x	
HM00048	HERA000073	HM00048										x				x	
HM00049	HERA000073.1	HM00049										x				x	
HM00050	HERA000074	Shuttle craft										x				x	
HM00051	HERA000075	HM00051										x				x	
HM00052	HERA000076	HM00052					x					x				x	

770 Yb^l, within the previously mapped Yb interval¹². Sb^l, within the previously mapped Sb
 771 interval¹². Sb controls a white/yellow hindwing margin and is not investigated in this study.
 772 The N locus has not been fine-mapped previously. A^{Yb}, number of above background SNPs

773 associated with the hindwing yellow bar in this study. A^N , number of above background
 774 SNPs associated with the forewing yellow band in this study. E^l , detected as differentially
 775 expressed between Hm aglaope and amaryllis from RNAseq data in this study
 776 (Supplementary Information). E^{gw} , detected as differentially expressed between forewing
 777 regions in the gene array in this study. E^{gr} , detected as differentially expressed between Hm
 778 plesseni and malleti in in the gene array in this study. E^{tw} , numbers of probes showing
 779 differential expression between forewing regions in the tiling array in this study. E^{tr} ,
 780 numbers of probes showing differential expression between Hm plesseni and malleti in in the
 781 tiling array in this study. Cr^l , within the previously mapped HeCr interval¹¹. A^{pet} , number of
 782 SNPs fixed for the alternative allele in He demophoon. A^{fav} , number of SNPs fixed for the
 783 alternative allele in He favorinus. P^l , within the previously mapped P interval¹³. A^{bic} , number
 784 of above background SNPs associated with the Hn bicoloratus phenotype in this study.
 785

786 Extended Data Table 2. Locations of fixed/above background SNPs and differentially
 787 expressed (DE) tiling array probes

		Positions of SNPs in the <i>He</i> and <i>Hn</i> association analyses				TEs	Other genes (exons or introns)	Other intergenic	Total	
		<i>cortex</i> coding exons	<i>cortex</i> UTR exons	<i>cortex</i> introns (nonTE)	<i>cortex</i> flanking intergenic (nonTE)					
<i>erato favorinus</i> fixed		2	0	96	8	2	0	0	108	
<i>erato demophoon</i> fixed		0	0	1	5	1	2	6	15	
<i>numata bicoloratus</i> above background		1	3	47	16	0	2	0	69	
Positions of DE tiling array probes		Known <i>cortex</i> coding exons	<i>cortex</i> UTR exons	<i>cortex</i> introns (nonTE)	miRNAs	TEs	Other gene exons	Other introns/ intergenic	Total	
Day3	malleti vs plesseni	Forewing proximal	8	7	323	0	13	1	7	359
		Forewing distal	12	2	327	0	8	0	8	357
		Hindwing	5	14	378	0	9	1	6	413
	Proximal vs distal	malleti	0	1	68	0	0	0	12	81
		plesseni	2	4	222	0	10	0	4	242
	Day1	malleti vs plesseni	Forewing proximal	1	0	22	0	3	0	7
Forewing distal			2	3	116	1	9	5	112	248
Hindwing			9	10	500	1	20	2	80	622
Proximal vs distal		malleti	0	12	95	0	1	0	0	108
		plesseni	3	3	81	0	99	0	0	186

788

789

790 Extended Data Table 3. SNPs showing the strongest phenotypic associations in the H.
 791 melpomene/timareta/silvaniform comparison.

Species	Race	Sample Code	SNP pos HW 457083† bar (p=6.07E- 10)	SNP pos 439063* (p=1.72E- 09)	SNP pos 602131‡ (p=2.42E- 09)	SNP pos 457056† (p=2.42E- 09)	FW band	SNP pos 584465§ (p=1.37E- 07)	SNP pos 584418§ (p=1.41E- 07)	SNP pos 584633§ (p=2.10E- 07)	SNP pos 603344‡ (p=2.19E- 07)
<i>H. melpomene</i>	<i>aglaope</i>	09-246	0 A/A	A/G	A/A	C/C	1	T/T	A/A	NA	T/T
<i>H. melpomene</i>	<i>aglaope</i>	09-267	0 A/A	G/G	A/A	C/C	1	T/T	A/A	C/C	T/T
<i>H. melpomene</i>	<i>aglaope</i>	09-268	0 A/A	G/G	A/A	C/C	1	T/T	A/A	C/C	T/T
<i>H. melpomene</i>	<i>aglaope</i>	09-357	0 A/A	G/G	G/A	C/C	1	T/T	NA	C/C	T/T
<i>H. melpomene</i>	<i>aglaope</i>	aglaope.1	0 A/A	G/G	NA	C/C	1	C/T	T/A	T/C	T/T
<i>H. melpomene</i>	<i>amandus</i>	2221	1 A/A	NA	G/G	C/C	0	C/C	T/T	T/T	A/A
<i>H. melpomene</i>	<i>amandus</i>	2228	1 A/A	NA	G/G	C/C	0	C/T	T/A	T/C	A/A
<i>H. melpomene</i>	<i>amaryllis</i>	09-332	1 T/T	A/A	G/G	T/T	0	C/C	T/T	T/T	A/A
<i>H. melpomene</i>	<i>amaryllis</i>	09-333	1 T/T	A/A	G/G	T/T	0	C/C	T/T	T/T	A/A
<i>H. melpomene</i>	<i>amaryllis</i>	09-075	1 T/T	A/A	G/G	T/T	0	C/C	T/T	T/T	A/A
<i>H. melpomene</i>	<i>amaryllis</i>	09-079	1 T/T	A/A	G/G	T/T	0	C/C	T/T	T/T	A/A
<i>H. melpomene</i>	<i>amaryllis</i>	amaryllis.1	1 T/T	A/A	G/G	T/T	0	C/C	T/T	T/T	A/A
<i>H. melpomene</i>	<i>bellula</i>	228	1 T/T	NA	G/G	T/T	0	C/C	T/T	T/T	NA
<i>H. melpomene</i>	<i>bellula</i>	231	1 T/T	NA	G/A	T/T	0	C/T	T/A	T/C	NA
<i>H. melpomene</i>	<i>cythera</i>	2856	1 T/T	A/A	G/G	T/T	0	C/C	T/T	T/T	A/A
<i>H. melpomene</i>	<i>cythera</i>	2857	1 NA	NA	NA	NA	0	NA	NA	NA	NA
<i>H. melpomene</i>	<i>malleti</i>	17162	0 A/A	G/G	A/A	C/C	1	T/T	A/A	C/C	T/T
<i>H. melpomene</i>	<i>melpomene</i>	18038	0 A/A	G/G	G/G	C/C	0	C/C	T/T	T/T	A/A
<i>H. melpomene</i>	<i>melpomene</i>	18097	0 NA	G/G	NA	C/C	0	C/C	T/T	T/T	NA
<i>H. melpomene</i>	<i>melpomenem</i>	0.06	0 A/A	G/G	G/G	C/C	0	C/C	T/T	T/T	A/A
<i>H. melpomene</i>	<i>melpomenegen_ref</i>		0 A/A	G/G	NA	C/C	0	C/C	T/T	T/T	A/A
<i>H. melpomene</i>	<i>melpomene</i>	13435	0 A/A	G/G	A/A	C/C	0	C/C	T/T	T/T	A/A
<i>H. melpomene</i>	<i>melpomene</i>	9315	0 A/A	G/G	A/A	C/C	0	C/C	T/T	T/T	A/A
<i>H. melpomene</i>	<i>melpomene</i>	9316	0 A/A	G/G	A/A	C/C	0	C/C	T/T	T/T	A/A
<i>H. melpomene</i>	<i>melpomene</i>	9317	0 A/A	G/G	A/A	C/C	0	C/C	T/T	T/T	A/A
<i>H. melpomene</i>	<i>plesseni</i>	9156	0 A/A	G/G	A/A	C/C	0	C/C	T/T	T/T	NA
<i>H. melpomene</i>	<i>plesseni</i>	16293	0 A/A	G/G	A/A	C/C	0	C/C	T/T	T/T	NA
<i>H. melpomene</i>	<i>rosina</i>	rosina.1	1 T/T	A/A	G/G	T/T	0	C/C	T/T	T/T	A/A
<i>H. melpomene</i>	<i>rosina</i>	2071	1 T/T	A/A	G/G	T/T	0	C/C	T/T	T/T	A/A
<i>H. melpomene</i>	<i>rosina</i>	531	1 T/T	A/A	G/G	T/T	0	C/C	T/T	T/T	A/A
<i>H. melpomene</i>	<i>rosina</i>	533	1 T/T	NA	G/G	T/T	0	C/C	T/T	T/T	NA
<i>H. melpomene</i>	<i>rosina</i>	546	1 T/T	A/A	G/G	T/T	0	C/C	T/T	T/T	A/A
<i>H. melpomene</i>	<i>thelxiopeia</i>	13566	0 A/A	G/G	A/A	C/C	1	C/T	T/A	T/C	T/T
<i>H. melpomene</i>	<i>vulcanus</i>	14632	1 T/T	A/A	G/G	T/T	0	C/C	T/T	T/T	NA
<i>H. melpomene</i>	<i>vulcanus</i>	519	1 T/T	A/A	G/G	T/T	0	C/C	T/T	T/T	A/A
<i>H. timareta</i>	<i>florencia</i>	2403	0 A/A	G/G	A/A	C/C	1	T/T	A/A	C/C	T/T
<i>H. timareta</i>	<i>florencia</i>	2406	0 A/A	A/G	A/A	C/C	1	T/T	A/A	C/C	T/T
<i>H. timareta</i>	<i>florencia</i>	2407	0 A/A	A/G	A/A	C/C	1	T/T	A/A	C/C	T/T
<i>H. timareta</i>	<i>florencia</i>	2410	0 A/A	G/G	A/A	C/C	1	T/T	A/A	C/C	T/T
<i>H. timareta</i>	<i>timareta</i>	8533	0 A/A	G/G	A/A	C/C	1	C/T	T/A	T/C	T/T
<i>H. timareta</i>	<i>timareta</i>	9184	0 A/A	G/G	A/A	C/C	1	T/T	A/A	C/C	T/T
<i>H. timareta</i>	<i>timareta</i>	8520	0 A/A	G/G	A/A	C/C	1	T/T	A/A	C/C	T/T
<i>H. timareta</i>	<i>timareta</i>	8523	0 A/A	G/G	A/A	C/C	1	T/T	A/A	C/C	T/T
<i>H. timareta</i>	<i>thelxinoe</i>	09-312	1 T/T	A/A	G/G	T/T	0	C/C	T/T	T/T	A/A
<i>H. timareta</i>	<i>thelxinoe</i>	8624	1 T/T	A/A	G/G	T/T	0	C/C	T/T	T/T	A/A
<i>H. timareta</i>	<i>thelxinoe</i>	8628	1 T/T	A/A	G/G	T/T	0	C/C	T/T	T/T	A/A
<i>H. timareta</i>	<i>thelxinoe</i>	8631	1 T/T	A/A	G/G	T/T	0	C/C	T/T	T/T	A/A
<i>H. elevatus</i>		09-343	0 A/T	G/G	A/A	T/T	1	C/T	NA	C/C	T/T
<i>H. pardalinus</i>	<i>sergestus</i>	09-326	0 A/A	A/A	A/A	NA	0	C/C	T/T	T/T	NA

792

793 *downstream of cortex, †between exons 3 and 4 of cortex, ‡upstream of cortex, §between

794 exons U4 and U3 of cortex. None of these SNPs are within known TEs. Colours show

795 phenotypic associations: yellow = yellow hindwing bar; pink = no yellow hindwing bar;

796 green = yellow forewing band; blue = no yellow forewing band; grey = allele does not match
 797 expected pattern.

798

799 Extended Data Table 4. Transposable Elements (TEs) found within the Yb region.

Unique Occurrences					No.	TE name	Superfamily		Type
BAC	mel	ros	ama	agl					
1					1	BEL-1	BEL		LTR retrotransposon
	1				1	CR1-2	Jockey	LINE	Non-LTR retrotransposon
					1	Daphne-1	Jockey	LINE	Non-LTR retrotransposon
1					1	Daphne-6	Jockey	LINE	Non-LTR retrotransposon
1					1	DNA-like-8			DNA transposon
	1	2			1	Helitron-like-14	Helitron_A		DNA transposon
	2				4	Helitron-like-12	Helitron_A		DNA transposon
	1				5	Helitron-like-12b	Helitron_A		DNA transposon
	1	1	1	1	7	Helitron-like-4a	Helitron_A		DNA transposon
						Helitron-like-4b	Helitron_A		DNA transposon
						Helitron-N2	Helitron_A		DNA transposon
					3	Helitron-like-7	Helitron_A		DNA transposon
5	3	3	1	2	16	Helitron-like-6a	Helitron_B		DNA transposon
						Helitron-like-6b	Helitron_B		DNA transposon
						Helitron-like-11	Helitron_B		DNA transposon
2	2	1		1	11	Helitron-like-15	Helitron_B		DNA transposon
6	5	3	1		18	Helitron-like-5	Helitron_B		DNA transposon
		1			2	Hmel_Unknown_50			
	1		1		2	Hmel_Unknown_174a/b			
	1				1	Hmel_Unknown_187b			
			1	1	2	Hmel_Unknown_230			
					1	Hmel_Unknown_234a			
					1	Hmel_Unknown_236a			
	1				1	Jockey-4	Jockey	LINE	Non-LTR retrotransposon
	1				1	LTR-3_gypsy	Gypsy		LTR retrotransposon
				1	1	Mariner-4	Mariner/Tc1		DNA transposon
1				3	29	Metulj-0	Metulj	SINE	Non-LTR retrotransposon
						Metulj-1	Metulj	SINE	Non-LTR retrotransposon
						Metulj-2	Metulj	SINE	Non-LTR retrotransposon
						Metulj-3	Metulj	SINE	Non-LTR retrotransposon
						Metulj-4	Metulj	SINE	Non-LTR retrotransposon
						Metulj-5	Metulj	SINE	Non-LTR retrotransposon
						Metulj-6	Metulj	SINE	Non-LTR retrotransposon
						Metulj-7	Metulj	SINE	Non-LTR retrotransposon
						nTc3-4	Mariner/Tc1		DNA transposon
						SINE-1	SINE	SINE	Non-LTR retrotransposon
1	1				2	nMar-3	Mariner/Tc1		DNA transposon
1					1	nMar-16	Mariner/Tc1		DNA transposon
			1		1	nMar-12/20	Mariner/Tc1		DNA transposon
				1	1	nPIF-3	PIF/Harbinger		DNA transposon
1					1	nTc3-2	Mariner/Tc1		DNA transposon
1					2	nTc3-3	Mariner/Tc1		DNA transposon
	1				2	R4-1	R2	LINE	Non-LTR retrotransposon
			1	1	6	Rep-1	REP	LINE	Non-LTR retrotransposon
		1		1	4	RTE-3	RTE	LINE	Non-LTR retrotransposon
2				1	2	RTE-11	RTE	LINE	Non-LTR retrotransposon
	1				3	Zenon-1	Jockey	LINE	Non-LTR retrotransposon
			1		1	Zenon-3	Jockey	LINE	Non-LTR retrotransposon

800